

Director

SECRET

SECURITY CLASSIFICATION OF THIS PAGE (When Data Entered)

| REPORT DOCUMENTATION PAGE | | READ INSTRUCTIONS BEFORE COMPLETING FORM |
|---|---|---|
| 1. REPORT NUMBER NRL Memorandum Report 4559 | 2. GOVT ACCESSION NO. AD-A107631 | 3. RECIPIENT'S CATALOG NUMBER |
| 4. TITLE (and Subtitle) COMPLEX ROOT-FINDING PROGRAM WITH APPLICATION TO THE DISPERSION RELATION OF WAVES PROPAGATING IN A FLUID-LOADED PLATE | 5. TYPE OF REPORT & PERIOD COVERED Interim report on a continuing problem. | |
| | 6. PERFORMING ORG. REPORT NUMBER | |
| 7. AUTHOR(s) P. S. Dubbelday* | 8. CONTRACT OR GRANT NUMBER(s) N00173-79-D-0004 SPI-8013287 | |
| 9. PERFORMING ORGANIZATION NAME AND ADDRESS Underwater Sound Reference Detachment Naval Research Laboratory P.O. Box 8337, Orlando, FL 32856 | 10. PROGRAM ELEMENT, PROJECT, TASK AREA & WORK UNIT NUMBERS 61153N; RR011-08-42; 0585-00 | |
| 11. CONTROLLING OFFICE NAME AND ADDRESS | 12. REPORT DATE November 20, 1981 | |
| | 13. NUMBER OF PAGES 50 | |
| 14. MONITORING AGENCY NAME & ADDRESS (if different from Controlling Office) | 15. SECURITY CLASS. (of this report) UNCLASSIFIED | |
| | 15a. DECLASSIFICATION/DOWNGRADING SCHEDULE | |
| 16. DISTRIBUTION STATEMENT (of this Report) Approved for public release; distribution unlimited. | | |
| 17. DISTRIBUTION STATEMENT (of the abstract entered in Block 20, if different from Report) | | |
| 18. SUPPLEMENTARY NOTES *The major part of this work was performed under a National Science Foundation Grant (SPI-8013287) by Dr. Dubbelday in his position as Professor of Physics at the Florida Institute of Technology. It was completed by him as an Oak Harbour Marine Associates employee under contract N00173-79-D-0004 to USRD. | | |
| 19. KEY WORDS (Continue on reverse side if necessary and identify by block number) Complex root finder Waves in fluid-loaded plate Complex roots of dispersion relation | | |
| 20. ABSTRACT (Continue on reverse side if necessary and identify by block number) -A method of finding complex roots is described, applicable to the situation where the given equation depends on a parameter in such a way that there exists a real root for a certain value of this parameter. This real root should be determined first by a real root-finding routine. By incrementing the parameter by adjustable steps to the desired value one can follow the progression of the corresponding root from the real axis into the complex plane. Alternately, one may apply this method to the case where it is desired to refine an approximate complex root obtained by other means, or track its progression through (Continues) | | |

DD FORM 1473
1 JAN 73

EDITION OF 1 NOV 65 IS OBSOLETE
S/N 0102-014-6601

SECURITY CLASSIFICATION OF THIS PAGE (When Data Entered)

315950

20 ABSTRACT (Continued)

the complex plane when a parameter of the equation is varied. The method is a two-dimensional counterpart to the one-dimensional technique whereby the change of sign of the pertinent function delimits the location of a root. The complex root is similarly enclosed in a nested set of squares of diminishing size. The method is illustrated by a typical example, the dispersion relation for the propagation of straight-crested waves in a homogeneous plate. Without fluid loading the propagation speed is real; loading the plate by a fluid moves this real root into the complex plane, which physically corresponds to the appearance of radiation into the fluid. The real and imaginary parts of the relative wave speed are presented, calculated according to exact elasticity theory and thick-plate theory, for antisymmetric and symmetric waves separately and simultaneously, as a function of the dimensionless wave number. Flow diagram, source program listing, and computation examples of the FORTRAN program are given.

CONTENTS

INTRODUCTION 1

COMPLEX ROOT FINDER: BASIC ALGORITHM 2

APPLICATION OF COMPLEX ROOT FINDER TO THE DISPERSION RELATION OF
STRAIGHT-CRESTED WAVES IN A FLUID-LOADED PLATE 5

 Theory of Plane-Crested Waves in a Fluid-Loaded Plate 5

 Dispersion Relations From Exact Elasticity Theory 5

 Dispersion Relations from Thick-Plate Theory 11

 Discussion of Results 12

REFERENCES 13

APPENDIX A - Description of Root-Finding Program 23

APPENDIX B - Flow Diagram 27

APPENDIX C - List of Major Symbols in FORTRAN Program 35

APPENDIX D - Source Program Listing 39

APPENDIX E - Examples 45

A

COMPLEX ROOT-FINDING PROGRAM WITH APPLICATION TO THE DISPERSION RELATION
OF WAVES PROPAGATING IN A FLUID-LOADED PLATE

INTRODUCTION

To find complex roots of an equation one often starts from the "principle of the argument", which can be stated as follows [1]:

"Let $f(z)$ be analytic within and on a simple closed contour C , except possibly for a finite number of poles inside C . If $f(z)$ does not vanish on C , then

$$\left(\frac{1}{2\pi}\right) \Delta_C \arg f(z) = Z - P \quad (1)$$

where $\Delta_C \arg f(z)$ is the total change in the argument of $f(z)$ around C , going in the counterclockwise direction, Z is the number of zeros, and P is the number of poles inside C . In counting the number of zeros and poles a zero of order m is counted m times, and a pole of order n is counted n times."

If it is known that there are no poles of $f(z)$ inside C this theorem is obviously useful in finding areas of limited extent in the complex plane where zeros are located. In practice problems arise in choosing the step size sufficiently fine so that no zeros are missed due to the ambiguity in the argument of a complex variable. This is discussed in reference 2. To determine the location of the zero more accurately, one might go through a succession of smaller contours--or rather use some other approximation scheme, as for instance the Newton-Raphson method [3].

In this study a different method of root finding is introduced. This method may be considered as a complex counterpart to a familiar root-finding technique for real functions. In the real case one looks for intervals where the value of the function changes sign. By repeatedly subdividing the interval and looking for changes in sign of the function, one may determine the root to any desired degree of precision. In the present routine the complex root is approximated by a sequence of squares of diminishing size, within which the root is known to be located. The basic algorithm is dependent on the fact that in the neighborhood of a zero of order one a complex function can be approximated by

$$f(z) = C(z - Z), \quad (2)$$

where C is a complex constant and Z is the given root. To obtain a first approximation for the given root one might rely on the principle of the argument, Eq. (1). It appears more attractive, though, to make use of the observation that in many practical cases the function $f(z)$ has a specific structure. Often the function $f(z)$ depends on a parameter r in such a way

that for $r = 0$ the function is real and has a real root, which can be found by a root finder for real roots. An example is the dispersion relation for straight-crested waves in plates. Without fluid loading the propagation speed is real. Fluid loading causes an imaginary part to appear, which corresponds to the phenomenon of sound radiation into the fluid. The fluid density features as the parameter r in this case. By increasing r in steps from zero to the nominal value one can follow the march of the root from the real axis into the complex plane. The step size can always be chosen small enough such that the approximation, Eq. (2), is sufficiently close. The root found at a given value for r is the seed for the determination of the root at the next larger value for r . It is clear that in this method one cannot find those roots that do not have a counterpart in the real case, as is true for some waves traveling at the interface of a plate and adjacent fluid. On the other hand, it has the advantage that a given complex root is identified by its place of origin on the real axis. Thus, there is no difficulty in establishing the signature of a root. The identification of complex roots from a random set in the plane and the sorting out of those roots that are organically related can pose a serious problem that is avoided by the present method.

In the second part of this report a typical application of the root-finding method is described. The pertinent equation is the dispersion relation of straight-crested waves propagating in a fluid-loaded plate. Both the dispersion relations following from exact elasticity theory and those that are based on thick-plate theory are used.

COMPLEX ROOT FINDER: BASIC ALGORITHM

Let $F(z,r)$ be the function, the root(s) of which is to be determined; r is a parameter such that, for $r = 0$, $F(z,0)$ is real and has a real root. Suppose that one has two points z_1 and z_2 close enough to the root Z of the function $F(z,r)$ that the linear approximation, Eq. (2), is applicable.

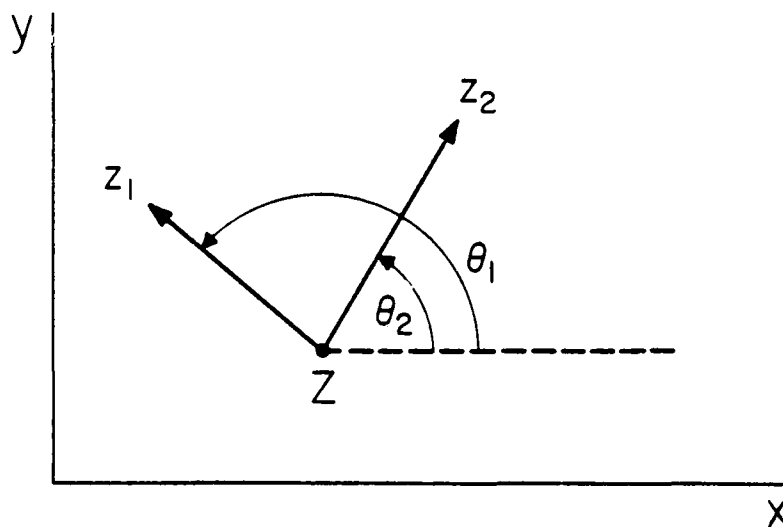


Fig. 1. Relative location of test pair z_1, z_2 and root Z

One sees in Fig. 1 that the angle $\theta = \theta_1 - \theta_2$ between the vectors from Z to the points z_1 and z_2 , respectively, in the complex plane is in the first or second quadrant when the loop $Z \rightarrow z_1 \rightarrow z_2$ is clockwise, and in the third or fourth quadrant if this loop is counterclockwise. The angle θ is determined by

$$\theta = \theta_1 - \theta_2 = \arg \frac{z_1 - Z}{z_2 - Z}. \quad (3)$$

Since the sine function is positive in the first and second quadrants and negative otherwise, it is clear that the location of Z with respect to the line through z_1 and z_2 is determined by the sign of the imaginary part of $(z_1 - Z)/(z_2 - Z)$. Another way of interpreting this criterion is to form the vector product of the complex numbers $(z_1 - Z)$ and $(z_2 - Z)$, considered as two-dimensional vectors, given by $(z_2 - Z)_x(z_1 - Z)_y - (z_2 - Z)_y(z_1 - Z)_x$. The algebraic sign of this vector product depends on the orientation of the loop $Z \rightarrow z_1 \rightarrow z_2$, and also has the same sign as the imaginary part of $(z_1 - Z)/(z_2 - Z)$. If z_1 and z_2 are close to Z the following approximation will be valid:

$$\begin{aligned} \operatorname{Im} \frac{z_1 - Z}{z_2 - Z} &= \operatorname{Im} \frac{C(z_1 - Z)}{C(z_2 - Z)} \\ &\cong \operatorname{Im} \frac{F(z_1, r)}{F(z_2, r)} \\ &= \frac{\operatorname{Im} F(z_1, r) \operatorname{Re} F(z_2, r) - \operatorname{Im} F(z_2, r) \operatorname{Re} F(z_1, r)}{|F(z_2, r)|^2}, \end{aligned} \quad (4)$$

where Re and Im indicate the real and imaginary parts of a complex number. Therefore, the algebraic sign of the expression in the numerator of the last part of Eq. (4)

$$S = \operatorname{Im} F(z_1, r) \operatorname{Re} F(z_2, r) - \operatorname{Im} F(z_2, r) \operatorname{Re} F(z_1, r) \quad (5)$$

determines the location of the root Z with respect to the test pair z_1, z_2 . Using the words horizontal and vertical to indicate the direction of the real and imaginary axes, respectively, one can describe the core of the root-finding procedure as follows. From an initial seed z_S close to the desired root a vertical test pair is created, namely two complex numbers z_1, z_2 with the same real part as the seed but differing by a small step size δ_0 , up and down from the seed. Thus,

$$z_1 = z_S + i\delta_0$$

and

$$z_2 = z_S - i\delta_0. \quad (6)$$

This test pair is moved horizontally by steps δ_0 until the expression S , indicated here by S_H , of Eq. (5) changes sign. A similar procedure is performed with a horizontal test pair, z_3, z_4 , determined by

$$z_3 = \frac{1}{2}(z_1+z_2) - \delta_0$$

and

$$z_4 = \frac{1}{2}(z_1+z_2) + \delta_0 \quad (7)$$

where δ_0 is the given step size and z_1, z_2 is the last vertical test pair, after S_H changed sign. The pertinent quantity S_V is now given by

$$S_V = \text{Im } F(z_3, r) \text{Re } F(z_4, r) - \text{Im } F(z_4, r) \text{Re } F(z_3, r). \quad (8)$$

This test pair is moved vertically by steps of the same size until S_V changes sign. Then the cycle is repeated with step size $\delta_1 = \delta_0/10$, etc. until the desired precision is reached. The subsequent vertical test pairs are formed by setting

$$z_1 = \frac{1}{2}(z_3+z_4) - i\delta_n$$

and

$$z_2 = \frac{1}{2}(z_3+z_4) + i\delta_n, \quad (9)$$

where $\delta_{n+1} = \delta_n/10$, and z_3, z_4 is the horizontal test pair obtained after S_V changed sign. The movement of the test pairs according to Eqs. (7) and (9) assures that they are at all times as close to the root Z as possible in view of the latest approximation.

The initial step size δ_0 is determined in relation to the change in the parameter r by a linear approximation of the function $F(z, r)$. At the $(i+1)$ th step one can set approximately

$$F(z_{i+1}, r_{i+1}) \cong \left(\frac{\partial F}{\partial z} \right)_i \delta z + \left(\frac{\partial F}{\partial r} \right)_i \Delta r, \quad (10)$$

where Δr is the step in the parameter r , and this linear expression is used to determine δz . The partial derivative $(\partial F/\partial r)_i$ is approximated by

$$\left(\frac{\partial F}{\partial r} \right)_i \cong \frac{F(z_i, r_i + \Delta r) - F(z_i, r_i)}{\Delta r} \quad (11)$$

and the partial derivative $(\partial F/\partial z)_i$ is approximated by

$$\left(\frac{\partial F}{\partial z} \right)_i \cong \frac{F(z_i + \Delta z, r_i) - F(z_i, r_i)}{\Delta z}. \quad (12)$$

The quantity Δz used to compute this difference quotient is read into the program, but it is found not to be critical. One may choose it to be, say, one percent of the nominal value of $|Z|$. The step size is thus given by

$$\delta z = - \frac{F(z_i, r_i + \Delta r) \Delta z}{F(z_i + \Delta z, r_i)}. \quad (13)$$

This step δz is complex; a real step size δ_0 is found by taking the maximum of the real and imaginary parts of δz . It was observed in practice that

the step size found in this way is not always adequate. Therefore, a step-size factor is read into the program. It is routinely set equal to one, but if the program does not converge rapidly one may enter a different step size to remedy this.

APPLICATION OF COMPLEX ROOT FINDER TO THE DISPERSION RELATION OF STRAIGHT-CRESTED WAVES IN A FLUID-LOADED PLATE

Theory of Plane-Crested Waves in a Fluid-Loaded Plate

It is possible to find solutions to the wave equations for infinite plates that are straight-crested waves propagating parallel to the faces of the plate. When exact linear elasticity theory is applied, these waves are known as Lamb waves. In this report the development of the theory by Viktorov [4] is followed. According to the outward appearance of the waves, one distinguishes antisymmetric and symmetric waves, which corresponds to different parity of the field variables as a function of the coordinate perpendicular to the faces of the plate. If the boundary conditions are the same at both faces of the plate (if the plate is loaded by the same fluid on both sides), the two wave types may occur separately. If such is not the case, the two types occur simultaneously.

Since exact elasticity theory leads to considerable complexity for other than the simplest geometries, approximate plate theories have been developed, known as thick-plate theories. Thick-plate theory for antisymmetric waves is described in reference 5, and thick-plate theory for symmetric waves is described in reference 6.

In the present study, the root finder is applied to dispersion relations from both exact theory and thick-plate theory. Moreover, in each case, one may select the root that originates in an antisymmetric or in a symmetric wave for an unloaded plate. Another option is to choose a fluid loaded on one side, or on both sides with the same fluid. Although strictly speaking the boundary conditions are not satisfied for the case where a wave of either antisymmetric or symmetric character is present by itself in a plate loaded on one side only, one may select these options in the program.

Dispersion Relations From Exact Elasticity Theory

The waves are propagating in a plate of thickness $2d$. The symbol c indicates phase speed, k is the wave number, and the subscripts d and s refer to dilatational waves and shear waves, respectively. For the sake of generality, it is assumed that waves in the fluid are incident in the plate. The waves can be most advantageously expressed in terms of the potentials ϕ and ψ in the form

$$\begin{aligned} \phi &= [A_d \cosh(qz) + B_d \sinh(qz)] \exp[i(\omega t - kx)] \\ \text{and} \\ \psi &= [D_s \sinh(sz) + C_s \cosh(sz)] \exp[i(\omega t - kx)] \end{aligned} \quad (14)$$

where x and z are coordinates in the direction of and perpendicular to the faces of the plate. The phase speed c equals ω/k , where ω is the angular frequency, k is the wavenumber, and the symbols q and s are given by

$$q^2 = k^2 - k_d^2 = k^2[1 - (c/c_d)^2]$$

and

$$s^2 = k^2 - k_s^2 = k^2[1 - (c/c_s)^2], \quad (15)$$

where k_d and k_s are the dilatational and shear wave numbers, respectively,

$$k_d = \omega[\rho_s/(\lambda + 2G)]^{1/2} = k(c/c_d)$$

and

$$k_s = \omega(\rho_s/G)^{1/2} = k(c/c_s), \quad (16)$$

where λ is the first Lamb constant, G is the shear modulus, and ρ_s is the density of the plate material. The subscripts a and s in the amplitudes A_s , B_a , D_s , and C_a refer to the two possible types of Lamb waves, antisymmetric and symmetric. The displacement components u and w are derived from the potentials by

$$u = \frac{\partial \phi}{\partial x} - \frac{\partial \psi}{\partial z}$$

and

$$w = \frac{\partial \phi}{\partial z} + \frac{\partial \psi}{\partial x}. \quad (17)$$

The amplitudes are related through the boundary conditions, which are the values for the normal and shear stresses applied at the two faces of the plate. These stresses are found in terms of the amplitudes by means of the following equation

$$\begin{aligned} \sigma_x &= \lambda \epsilon + 2G \epsilon_x \\ \sigma_z &= \lambda \epsilon + 2G \epsilon_z \\ \sigma_{zx} &= G \epsilon_{zx}. \end{aligned} \quad (18)$$

The elements of the strain tensor are given in terms of the displacement vector of a particle with components u , v , w by

$$\begin{aligned} \epsilon_x &= \frac{\partial u}{\partial x} \\ \epsilon_z &= \frac{\partial w}{\partial z} \\ \epsilon_{zx} &= \frac{\partial w}{\partial x} + \frac{\partial u}{\partial z}. \end{aligned} \quad (19)$$

This leads to the following expressions for the stresses, using Eqs. (14) and (17) (the factor $\exp[i(\omega t - kx)]$ is suppressed)

$$\begin{aligned} \sigma_z = & G[A_s(k^2 + s^2)\cosh(qz) + B_a(k^2 + s^2) \sinh(qz) \\ & - C_a 2iks \sinh(sz) - D_s 2iks \cosh(sz)] \end{aligned} \quad (20)$$

$$\begin{aligned} \sigma_{zx} = & -G[A_s 2ikq \sinh(qz) + B_a 2ikq \cosh(qz) \\ & + C_a (k^2 + s^2)\cosh(sz) + D_s(k^2 + s^2)\sinh(sz)]. \end{aligned} \quad (21)$$

The applied stresses for a plate in vacuum are zero. In that case the anti-symmetric and symmetric waves independently satisfy the zero boundary conditions, and thus

$$B_a(k^2 + s^2) \sinh(qd) - C_a 2iks \sinh(sd) = 0$$

$$B_a 2ikq \cosh(qd) + C_a(k^2 + s^2)\cosh(sd) = 0$$

$$A_s (k^2 + s^2)\cosh(qd) - D_s 2iks \cosh(sd) = 0$$

and

$$A_s 2ikq \sinh(qd) + D_s(k^2 + s^2)\sinh(sd) = 0. \quad (22)$$

By elimination of the amplitudes from these equations, one arrives at the dispersion relations

$$(k^2 + s^2)^2 \sinh(qd)\cosh(sd) - 4k^2qs \cosh(qd)\sinh(sd) = 0 \quad (23)$$

for antisymmetric waves, and

$$(k^2 + s^2)^2\cosh(qd)\sinh(sd) - 4k^2qs \sinh(qd)\cosh(sd) = 0 \quad (24)$$

for symmetric waves. At large values of kd both dispersion relationships approach the same relation,

$$4k^2qs - (k^2 + s^2)^2 = 0, \quad (25)$$

which is the dispersion relation for Rayleigh waves defined as waves at the surface of a semi-infinite solid.

The space dependence of the (partial) pressures in the fluids is given by the following expressions. For the pressure p_i of the incident wave,

$$p_i = P_i \exp[-ik_0(x \sin\theta - z \cos\theta)]. \quad (26)$$

where k_0 is the wave number of the wave in the fluid. For the pressure p_r of the reflected wave,

$$p_r = P_r \exp[-ik_0(x \sin\theta + z \cos\theta)]. \quad (27)$$

For the pressure p_t of the transmitted wave,

$$p_t = P_t \exp[-ik'(x \sin\theta' - z \cos\theta')], \quad (28)$$

where k' is the wave number of the transmitted wave.

The angles θ and θ' are the angles of the incident and transmitted rays with the normal to the face of the plate, respectively. The total pressure in the fluid at the surface of the plate on the side of the incident wave is

$$p(z = d) = p_i + p_r = (P_o + P)\exp(-ikx), \quad (29)$$

where $P_o = P_i \exp(ik_o d \cos\theta)$ and $P = P_r \exp(-ik_o d \cos\theta)$. The pressure at the surface of the plate on the opposite side is

$$p(z = -d) = P'\exp(-ikx), \quad (30)$$

where $P' = P_t \exp(-ik'd \cos\theta')$. Here the coincidence condition is used, namely

$$k = k_o \sin\theta = k' \sin\theta'. \quad (31)$$

The following boundary conditions [Eqs. (32) through (38)] are applicable to the problem of wave propagation in a fluid-loaded plate. At the side of the incoming wave, where $z = d$, one has continuity of the normal stress σ_z and the shear stress $\sigma_{zx} = 0$. Thus, combining Eq. (20) with Eq. (29), and using Eq. (21), one has

$$\begin{aligned} G[A_s(k^2+s^2)\cosh(qd) + B_a(k^2+s^2)\sinh(qd) \\ - C_a 2iks \sinh(sd) - D_s 2iks \cosh(sd)] = - (P_o + P) \end{aligned} \quad (32)$$

and

$$\begin{aligned} A_s 2ikq \sinh(qd) + B_a 2ikq \cosh(qd) \\ + C_a (k^2+s^2)\cosh(sd) + D_s (k^2+s^2)\sinh(sd) = 0. \end{aligned} \quad (33)$$

In a similar fashion, one has two conditions for the stress at the opposite face, where $z = -d$, by combining Eq. (20) with Eq. (30), and using Eq. (21)

$$\begin{aligned} G[A_s(k^2+s^2)\cosh(qd) - B_a(k^2+s^2)\sinh(qd) \\ + C_a 2iks \sinh(sd) - D_s 2iks \cosh(sd)] = - P' \end{aligned} \quad (34)$$

and

$$\begin{aligned} - A_s 2ikq \sinh(qd) + B_a 2ikq \cosh(qd) \\ + C_a (k^2+s^2)\cosh(sd) - D_s (k^2+s^2)\sinh(sd) = 0. \end{aligned} \quad (35)$$

Also, at the interfaces, the component of the particle velocity in the solid in the z direction has to equal that in the fluid. This leads to the relation between pressure gradient in the fluid and particle acceleration in the solid at a boundary. In general, one has

$$-\frac{1}{\rho_0} \frac{\partial p}{\partial z} = \frac{\partial^2 w}{\partial t^2} \text{ (fluid)} = \frac{\partial^2 w}{\partial t^2} \text{ (solid)}, \quad (36)$$

where ρ_0 is the density of the fluid. This gives for $z = d$

$$-\omega^2 q A_s \sinh(qd) - \omega^2 B_a q \cosh(qd) + \omega^2 ik C_a \cosh(sd) + ik\omega^2 D_s \sinh(sd) = -ik(\cot\theta)(P_0 - P)/\rho_0, \quad (37)$$

and for $z = -d$

$$\omega^2 q A_s \sinh(qd) - \omega^2 q B_a \cosh(qd) + \omega^2 ik C_a \cosh(sd) - ik\omega^2 D_s \sinh(sd) = -ik(\cot\theta')P'/\rho_0. \quad (38)$$

The set of boundary conditions can be advantageously represented in the form of a matrix of the coefficients, given in Table I. The rows are indicated by the numbers of the equations, and the columns are marked by the corresponding dimensionless amplitudes for the displacements and pressures. The density ρ_0 applies to the fluid on the insonified side, ρ' is the density of the fluid on the other side of the plate. The relation $c_s^2 = G/\rho_s$ has been used to arrive at the given form of the matrix. Since the usual FORTRAN library routine for complex numbers carries only circular functions, a transformation is made whereby $s = is'$ and $q = iq'$. Then the hyperbolic functions are transformed into circular functions. The result is shown in Table II.

To find the dispersion relation for free waves in a plate loaded by fluid on one side only, one omits from the matrix the sixth row and the fifth and seventh columns and sets the determinant value of the remaining matrix equal to zero. The dispersion relation for waves in a plate loaded on one side is given by

$$i\Delta_a\Delta_s + (\rho_0/\rho_s)q'd(k_s d)^4 [\Delta_a \sin(q'd)\sin(s'd) - \Delta_s \cos(q'd)\cos(s'd)] / [2(kd)\cot\theta]. \quad (39)$$

If one indicates the matrix elements of Table II by m_{ij} , the symbols Δ_a, Δ_s are defined by $\Delta_a = m_{11}m_{22} - m_{12}m_{21}$, and $\Delta_s = m_{33}m_{44} - m_{34}m_{43}$.

The dispersion relation for a plate loaded on both sides by the same fluid is obtained by omitting column five from the matrix and setting the determinant value of the remaining matrix equal to zero. The density ρ' is replaced by ρ_0 and $\theta' = \theta$. This determinant can be factored in two parts, corresponding to antisymmetric waves and symmetric waves. The two dispersion relations are

$$i\Delta_a\Delta_s - (\rho_0/\rho_s)q'd(k_s d)^4 \Delta_s \cos(q'd)\cos(s'd) / [(kd)\cot\theta] = 0 \quad (40)$$

for antisymmetric waves, and

Table I. Matrix of coefficients of equations describing wave propagation in fluid-loaded plate in terms of hyperbolic functions. Exact elasticity theory.

| Field variables - B_a/d^2 | C_a/d^2 | A_s/d^2 | D_s/d | $P_0/(\rho_0 c_s^2)$ | $P/(\rho_0 c_s^2)$ | $P'/(\rho' c_s^2)$ |
|--------------------------------|-------------------------|------------------------|------------------------|--------------------------------------|-------------------------------------|---------------------------------------|
| (32) $(k^2+s^2)d \sinh(qd)$ | $-2iks^2 \sinh(sd)$ | $(k^2+s^2)d \cosh(qd)$ | $-2iksd \cosh(sd)$ | c_0/c_s | $-c_0/c_s$ | 0 |
| (33) $2ikqd \cosh(qd)$ | $(k^2+s^2)d \cosh(sd)$ | $2ikqd \sinh(qd)$ | $(k^2+s^2)d \sinh(sd)$ | 0 | 0 | 0 |
| (34) $-(k^2+s^2)d^2 \sinh(qd)$ | $2iksd \sinh(sd)$ | $(k^2+s^2)d \cosh(qd)$ | $-2iksd \cosh(sd)$ | 0 | 0 | c_0/c_s |
| (35) $-2ikqd \cosh(qd)$ | $-(k^2+s^2)d \cosh(sd)$ | $2ikqd \sinh(qd)$ | $(k^2+s^2)d \sinh(sd)$ | 0 | 0 | 0 |
| (37) $qd \cosh(qd)$ | $-ikd \cosh(sd)$ | $qd \sinh(qd)$ | $-ikd \sinh(sd)$ | $\frac{-ikd \cot \theta}{(k_s d)^2}$ | $\frac{ikd \cot \theta}{(k_s d)^2}$ | 0 |
| (38) $qd \cosh(qd)$ | $-ikd \cosh(sd)$ | $-qd \sinh(qd)$ | $ikd \sinh(sd)$ | 0 | 0 | $-\frac{ikd \cot \theta'}{(k_s d)^2}$ |

Table II. Matrix of coefficients of equations describing wave propagation in fluid-loaded plate in terms of circular functions. Exact elasticity theory.

| Field variables - B_a/d^2 | C_a/d^2 | A_s/d^2 | D_s/d^2 | $P_0/(\rho_0 c_s^2)$ | $P/(\rho_0 c_s^2)$ | $P'/(\rho' c_s^2)$ |
|--------------------------------|--|--------------------------|---------------------------|--------------------------------------|-------------------------------------|---------------------------------------|
| (32) $(k^2-s^2)d^2 \sin(q'd)$ | $2iks'd^2 \sin(s'd)$ | $(k^2-s^2)d^2 \cos(q'd)$ | $-2iks'd^2 \cos(s'd)$ | c_0/c_s | $-c_0/c_s$ | 0 |
| (33) $-21kq'd^2 \cos(q'd)$ | $-(k^2-s^2)d^2 \cos(s'd) + 21kq'd^2 \sin(q'd)$ | $-21kq'd^2 \sin(q'd)$ | $-(k^2-s^2)d^2 \sin(s'd)$ | 0 | 0 | 0 |
| (34) $-(k^2-s^2)d^2 \sin(q'd)$ | $-21ks'd^2 \sin(s'd)$ | $(k^2-s^2)d^2 \cos(q'd)$ | $-21ks'd^2 \cos(s'd)$ | 0 | 0 | c_0/c_s |
| (35) $+21kq'd^2 \cos(q'd)$ | $-(k^2-s^2)d^2 \cos(s'd) + 21kq'd^2 \sin(q'd)$ | $-21kq'd^2 \sin(q'd)$ | $-(k^2-s^2)d^2 \sin(s'd)$ | 0 | 0 | 0 |
| (37) $q'd \cos(q'd)$ | $-ikd \cos(s'd)$ | $-q'd \sin(q'd)$ | $-ikd \sin(s'd)$ | $-\frac{ikd \cot \theta}{(k_s d)^2}$ | $\frac{ikd \cot \theta}{(k_s d)^2}$ | 0 |
| (38) $q'd \cos(q'd)$ | $-ikd \cos(s'd)$ | $q'd \sin(q'd)$ | $ikd \sin(s'd)$ | 0 | 0 | $-\frac{ikd \cot \theta'}{(k_s d)^2}$ |

$$i\Delta_a\Delta_s + (\rho_o/\rho_s)q'd(k_s d)^4\Delta_a\sin(q'd)\sin(s'd)/[(kd)\cot\theta] = 0 \quad (41)$$

for symmetric waves. In a strict sense it is not possible to have the two wave types separately in a plate loaded on one side only, since the boundary conditions are not satisfied in that case. For comparison, one might still force the situation by altogether leaving out rows and columns belonging to one wave type or the other. That way two more dispersion relations are found for a plate loaded by a fluid on one side, namely

$$i\Delta_a\Delta_s - (\rho_o/\rho_s)q'd(k_s d)^4\Delta_s\cos(q'd)\cos(s'd)/[2(kd)\cos\theta] = 0 \quad (42)$$

for antisymmetric waves only, and

$$i\Delta_a\Delta_s + (\rho_o/\rho_s)q'd(k_s d)^4\Delta_a\sin(q'd)\sin(s'd)/[2(kd)\cos\theta] = 0 \quad (43)$$

for symmetric waves only.

Dispersion Relations From Thick-Plate Theory

The description of thick-plate theory for straight-crested waves in fluid-loaded plates is given in references 6 and 7. The matrix of the coefficients of the equations of motion and boundary conditions is given in Table III. The symbol γ indicates the phase speed c of the waves divided by the shear wave speed c_s . The subscripts p and d indicate extensional and dilatational waves, respectively. The correction factor for the effective shear modulus is κ_1 for flexural waves and κ_2 for extensional waves. U is the average displacement in the z direction in extensional waves, W is the average displacement in the x direction in flexural waves, χ is the average strain in the z direction in extensional waves, and ϕ_x is the average angle of rotation of a cross section in flexural waves.

The various possibilities of fluid loading are parallel to those in exact elasticity theory. The dispersion relation for a plate loaded by a fluid on one side is obtained from the matrix in Table III by omitting columns 5 and 7 and row 6. The determinant value of the resulting matrix is equated to zero resulting in

$$i\Delta_a'\Delta_s' - \frac{1}{2}\gamma^3(k_s d)(\rho_o/\rho_s)(\Delta_a' n_{33} + \Delta_s' n_{11})/\cot\theta = 0. \quad (44)$$

The matrix elements are indicated by n_{ij} , and further $\Delta_a' = n_{11}n_{22} - n_{12}n_{21}$, and $\Delta_s' = n_{33}n_{44} - n_{34}n_{43}$. Again, it is not theoretically possible to satisfy the boundary conditions for a plate loaded by a fluid on one side by antisymmetric wave or antisymmetric waves separately. For comparison, one might force the issue by just leaving out the pertinent lines from the matrix. This leads to the following dispersion relations. For antisymmetric waves, fluid on one side only one has

$$i\Delta_a' - \frac{1}{2}\gamma^3(k_s d)(\rho_o/\rho_s) n_{11}/\cot\theta = 0, \quad (45)$$

and for symmetric waves, fluid on one side only has

$$i\Delta_s' - \frac{1}{2}\gamma^3(k_s d)(\rho_o/\rho_s) n_{33}/\cot\theta = 0. \quad (46)$$

Table III - Matrix of coefficients of equations describing wave propagation by fluid-loaded plate in thick-plate theory

Field variables -

| ϕ_x | W/d | V/d | χ | $P_2/(\rho_0 c_s^2)$ | $P/(\rho_0 c_s^2)$ | $P'/(\rho_0 c_s^2)$ |
|---|---------------------------------------|---------------------------------|---|----------------------|--------------------|-----------------------------------|
| $\frac{1}{3}(kd)^2(\gamma^2 - \gamma_p^2) - \kappa_1^2$ | $i(kd)\kappa_1^2$ | 0 | 0 | 0 | 0 | 0 |
| $i(kd)\kappa_1^2$ | $(kd)^2$ $(\kappa_1^2 - \gamma^2)$ | 0 | 0 | $\rho_0/2\rho_s$ | $\rho_0/2\rho_s$ | $-\rho_0/2\rho_s$ |
| 0 | 0 | $(kd)^2(\gamma_d^2 - \gamma^2)$ | $i(kd)(\gamma_d^2 - 2)$ | 0 | 0 | 0 |
| 0 | 0 | $-i(kd)(\gamma_d^2 - 2)$ | $\frac{1}{3}(kd)^2(\kappa_2^2 - \gamma^2) + \gamma_d^2$ | $\rho_0/2\rho_s$ | $\rho_0/2\rho_s$ | $\rho_0/2\rho_s$ |
| 0 | $\gamma^2(kd)^2$ | 0 | $\gamma^2(kd)^2$ | $-i(kd)\cot\theta$ | $i(kd)\cot\theta$ | 0 |
| 0 | $\gamma^2(kd)^2$ | 0 | $-\gamma^2(kd)^2$ | 0 | 0 | $-i(kd)(\rho_0/\rho')\cot\theta'$ |

If the wave is loaded by the same fluid on both sides, the corresponding matrix is found from Table III by omitting column 5 and setting $\rho_0 = \rho'$ and $\theta = \theta'$. Then the determinant value of the matrix can be split in two factors for antisymmetric and symmetric waves separately--with the dispersion relations, for antisymmetric waves

$$i\Delta'_a - \gamma^3(k_s d)(\rho_0/\rho_s)n_{11}/\cot\theta = 0, \quad (47)$$

and for symmetric waves

$$i\Delta'_s - \gamma^3(k_s d)(\rho_0/\rho_s)n_{33}/\cot\theta = 0. \quad (48)$$

Discussion of Results

In this section results are discussed of the application of the root finder to wave propagation in plates. Only those complex roots are given that originate in zero order antisymmetric and symmetric Lamb waves in an

unloaded plate. The case of steel was chosen, with Poisson's ratio equal to 0.3028, a shear wave speed $c_s = 3264$ m/s, and water of 4°C temperature for which $c_0 = 1447$ m/s. The value of the Rayleigh wave speed relative to the shear wave speed in steel is 0.9278, and this was chosen as the value of the correction factor for the effective shear modulus in the thick-plate computations. The results for the various options are shown in Tables IV through VII. The results of the change in the real part of the relative wave speed $Re\gamma$ are not overly significant. First, the variation with frequency is partly due to the lack of accuracy of the real seed used in the program; thus no trends are visible. Secondly, the fractional change in $Re\gamma$ is very small. More important is the behavior of the imaginary part of γ . Two aspects of the results will be discussed: in the first place, just how noticeable is the effect of the presence of two wave types, symmetric and antisymmetric; and in the second place, how close are the approximations of the thick-plate theory to the results of exact elasticity theory?

In Figs. 2 and 3 a comparison is made between the results from exact elasticity theory for a plate loaded on one side by a fluid. In Fig. 2 the complex root originates in an antisymmetric wave in an unloaded plate. In Fig. 3 it derives from a symmetric wave in an unloaded plate. In both cases, Curve #1 represents the result of admitting both antisymmetric and symmetric waves to propagate in the plate. This is the correct way of satisfying the boundary conditions on each side of the plate. If one leaves out the second type of wave, the symmetric one in Fig. 1 and the antisymmetric one in Fig. 2, Curves #2 are obtained. The curves show that admitting both types of waves instead of only one gives a very small difference at lower values of the dimensionless wave number kd , but the difference becomes quite pronounced at higher values of kd , above $kd \approx 6$. At this value of kd , the wavelength is of the order of the thickness of the plate. The comparison of exact theory with thick-plate theory in Figs. 4 and 5 shows a corresponding behavior: the thick-plate theory gives results reasonably close to exact-plate theory, except in the region where the exact theory starts to display the influence of the complementary wave type, around $kd \approx 6$ or 7. Thus, even where the thick-plate theory admits both types of waves to take part in the propagation, it is not able to correctly predict the strong reduction in attenuation that occurs at higher values of kd according to the more reliable exact theory. In thick-plate theory there is very little change in γ when both types of waves are admitted as compared with one type only.

REFERENCES

1. J.W. Dettman, Applied Complex Variables (McMillan Co., New York, 1965) p 211.
2. Peter Ugincius, "Creeping-Wave Analysis of Acoustic Scattering by Elastic Cylindrical Shells," NWL Technical Report Tr-2128, Feb. 1968, p 57.
3. Ibid, p 58.
4. I.A. Viktorov, Rayleigh and Lamb Waves (Plenum Press, New York, 1967).

5. R.D. Mindlin, "Influence of Rotatory Inertia and Shear on Flexural Motions of Isotropic, Elastic Plates," Trans. ASME, Ser. E, J. Appl. Mech. 18, 31-38 (1951)
6. P.S. Dubbelday, "Effective Shear Modulus for Flexural and Extensional Waves in an Unloaded Thick Plate," NRL Report 8372, Sep 1980.
7. P.S. Dubbelday, "Contribution of Antisymmetric and Symmetric Waves to the Reflection of Sound in a Fluid by a Thick Homogeneous Plate," NRL Memorandum Report 4312, Oct 1980.
8. Clementina M. Ruggiero, "Solutions of Transcendental and Algebraic Equations with Application to Wave Propagation in Elastic Plates," NRL Memorandum Report 4449 (in preparation).

Table IV. Roots of dispersion relation in thick-plate theory corresponding to antisymmetric waves in unloaded plate.

| UNLOADED PLATE | | | LOADED PLATE | | | | | |
|----------------|----------|---------|--|---|--|---|--|---|
| | | | A+S, loaded one side | | A only, loaded one side | | A only, loaded both sides | |
| kd | γ | $k_g d$ | Re($\Delta\gamma$) | Im($\Delta\gamma$) | Re($\Delta\gamma$) | Im($\Delta\gamma$) | Re($\Delta\gamma$) | Im($\Delta\gamma$) |
| 0.7 | 0.5322 | 0.37254 | 3.04×10^{-4} $\pm 3 \times 10^{-6}$ | 2.0767×10^{-2} $\pm 3 \times 10^{-6}$ | 1.69×10^{-4} $\pm 3 \times 10^{-6}$ | 2.0775×10^{-2} $\pm 3 \times 10^{-6}$ | 1.72×10^{-4} $\pm 7 \times 10^{-6}$ | 4.0452×10^{-2} $\pm 7 \times 10^{-6}$ |
| 1.1 | 0.6758 | 0.74338 | -7.9×10^{-5} $\pm 2 \times 10^{-6}$ | 1.0965×10^{-2} $\pm 3 \times 10^{-6}$ | 1.83×10^{-4} $\pm 3 \times 10^{-6}$ | 1.0964×10^{-2} $\pm 3 \times 10^{-6}$ | -7.25×10^{-4} $\pm 5 \times 10^{-6}$ | 2.1885×10^{-2} $\pm 5 \times 10^{-6}$ |
| 1.5 | 0.7575 | 1.13625 | 1.9×10^{-5} $\pm 1 \times 10^{-6}$ | 8.243×10^{-3} $\pm 1 \times 10^{-6}$ | -9.1×10^{-5} $\pm 1 \times 10^{-6}$ | 8.233×10^{-3} $\pm 1 \times 10^{-6}$ | -3.79×10^{-4} $\pm 3 \times 10^{-6}$ | 1.6456×10^{-2} $\pm 3 \times 10^{-6}$ |
| 2.5 | 0.8496 | 2.12400 | 1.18×10^{-4} $\pm 1 \times 10^{-6}$ | 5.472×10^{-3} $\pm 1 \times 10^{-6}$ | 1.2×10^{-5} $\pm 1 \times 10^{-6}$ | 5.473×10^{-3} $\pm 1 \times 10^{-6}$ | 1.24×10^{-4} $\pm 3 \times 10^{-6}$ | 1.0946×10^{-2} $\pm 3 \times 10^{-6}$ |
| 4.5 | 0.9005 | 4.05135 | 1.568×10^{-4} $\pm 6 \times 10^{-7}$ | 3.3481×10^{-3} $\pm 6 \times 10^{-7}$ | 9.00×10^{-6} $\pm 2 \times 10^{-7}$ | 3.3512×10^{-3} $\pm 2 \times 10^{-7}$ | 3.5×10^{-5} $\pm 3 \times 10^{-6}$ | 6.699×10^{-3} $\pm 3 \times 10^{-6}$ |
| 6.5 | 0.9142 | 5.94230 | 1.07×10^{-4} $\pm 1 \times 10^{-6}$ | 2.392×10^{-3} $\pm 1 \times 10^{-6}$ | -4.72×10^{-5} $\pm 1 \times 10^{-7}$ | 2.3979×10^{-3} $\pm 1 \times 10^{-7}$ | -6.9×10^{-5} $\pm 1 \times 10^{-6}$ | 4.795×10^{-3} $\pm 1 \times 10^{-6}$ |
| 8.5 | 0.9197 | 7.81745 | 1.611×10^{-4} $\pm 5 \times 10^{-7}$ | 1.8515×10^{-3} $\pm 5 \times 10^{-7}$ | 5.1×10^{-6} $\pm 2 \times 10^{-7}$ | 1.86×10^{-3} $\pm 2 \times 10^{-7}$ | -8.1×10^{-6} $\pm 2 \times 10^{-7}$ | 3.722×10^{-3} $\pm 2 \times 10^{-7}$ |
| 10.1 | 0.9220 | 9.31220 | 1.893×10^{-4} $\pm 5 \times 10^{-7}$ | 1.5651×10^{-3} $\pm 5 \times 10^{-7}$ | 3.23×10^{-5} $\pm 2 \times 10^{-7}$ | 1.5750×10^{-3} $\pm 2 \times 10^{-7}$ | 2.24×10^{-5} $\pm 6 \times 10^{-7}$ | 3.1501×10^{-3} $\pm 6 \times 10^{-7}$ |

Steel, $\nu = 0.3028$ Water, $c_0 = 1447$ m/s
 $c_s = 3264$ m/s γ_R in steel = 0.9278

Table V. Roots of dispersion relation in exact elasticity theory corresponding to antisymmetric waves in unloaded plate.

| UNLOADED PLATE | | | LOADED PLATE | | | | | |
|----------------|----------|----------|--|---|---|---|--|---|
| kd | γ | k_{gd} | A+S, loaded one side | | A only, loaded one side | | A only, loaded both sides | |
| | | | Re($\Delta\gamma$) | Im($\Delta\gamma$) | Re($\Delta\gamma$) | Im($\Delta\gamma$) | Re($\Delta\gamma$) | Im($\Delta\gamma$) |
| 0.7 | 0.5338 | 0.37366 | 4.28×10^{-4} $\pm 1 \times 10^{-6}$ | 1.8792×10^{-2} $\pm 1 \times 10^{-6}$ | -5.906×10^{-3} | 1.8761×10^{-2} $\pm 1 \times 10^{-6}$ | -6.03×10^{-3} $\pm 1 \times 10^{-5}$ | 3.672×10^{-2} $\pm 1 \times 10^{-5}$ |
| 1.1 | 0.6801 | 0.74811 | 8.88×10^{-5} $\pm 5 \times 10^{-7}$ | 9.3676×10^{-3} $\pm 5 \times 10^{-7}$ | -9.8×10^{-6} $\pm 5 \times 10^{-7}$ | 9.3676×10^{-3} $\pm 5 \times 10^{-7}$ | -3.41×10^{-4} $\pm 1 \times 10^{-6}$ | 1.8709×10^{-2} $\pm 1 \times 10^{-6}$ |
| 1.5 | 0.7643 | 1.14645 | 9.16×10^{-5} $\pm 4 \times 10^{-7}$ | 6.8507×10^{-3} $\pm 4 \times 10^{-7}$ | -2.04×10^{-5} $\pm 4 \times 10^{-7}$ | 6.8519×10^{-3} $\pm 4 \times 10^{-7}$ | 1.084×10^{-4} $\pm 1 \times 10^{-7}$ | 1.3698×10^{-2} $\pm 1 \times 10^{-6}$ |
| 2.5 | 0.8601 | 2.15050 | 3.391×10^{-4} $\pm 3 \times 10^{-7}$ | 4.7823×10^{-3} $\pm 3 \times 10^{-7}$ | 1.582×10^{-4} $\pm 3 \times 10^{-7}$ | 4.7899×10^{-3} $\pm 3 \times 10^{-7}$ | 2.432×10^{-4} $\pm 5 \times 10^{-7}$ | 9.5788×10^{-3} $\pm 5 \times 10^{-7}$ |
| 4.5 | 0.9122 | 4.10490 | 7.486×10^{-4} $\pm 3 \times 10^{-7}$ | 4.0471×10^{-3} $\pm 3 \times 10^{-7}$ | 1.198×10^{-4} $\pm 2 \times 10^{-7}$ | 4.1106×10^{-3} $\pm 2 \times 10^{-7}$ | 3.256×10^{-4} $\pm 5 \times 10^{-7}$ | 8.2174×10^{-3} $\pm 5 \times 10^{-7}$ |
| 6.5 | 0.9240 | 6.00600 | 3.29×10^{-3} $\pm 2 \times 10^{-5}$ | 2.56×10^{-3} $\pm 2 \times 10^{-5}$ | 8.7082×10^{-3} $\pm 9 \times 10^{-7}$ | 4.2833×10^{-3} $\pm 9 \times 10^{-7}$ | 3.522×10^{-4} $\pm 2 \times 10^{-6}$ | 8.564×10^{-3} $\pm 2 \times 10^{-6}$ |
| 8.5 | 0.9269 | 7.87865 | 9.51×10^{-4} $\pm 2 \times 10^{-6}$ | 9.8×10^{-5} $\pm 2 \times 10^{-6}$ | 1.26×10^{-4} $\pm 2 \times 10^{-6}$ | 4.474×10^{-3} $\pm 2 \times 10^{-6}$ | 4.02×10^{-4} $\pm 2 \times 10^{-6}$ | 8.951×10^{-3} $\pm 2 \times 10^{-6}$ |
| 10.1 | 0.9267 | 9.36876 | 1.1495×10^{-3} 4×10^{-8} | 8.85×10^{-6} 4×10^{-8} | 9.57×10^{-4} $\pm 1 \times 10^{-6}$ | 4.549×10^{-3} $\pm 1 \times 10^{-6}$ | 1.22×10^{-3} $\pm 2 \times 10^{-6}$ | 9.102×10^{-3} $\pm 2 \times 10^{-6}$ |

Steel, $\nu = 0.3028$
 $c_s = 3264$ m/s

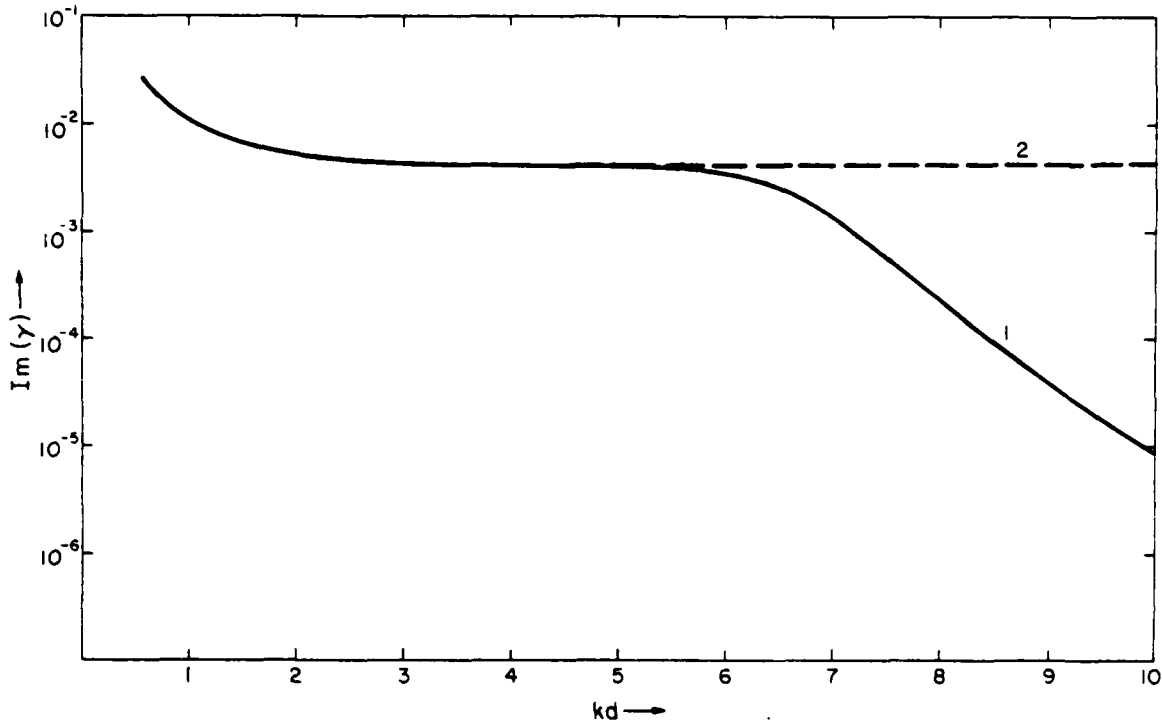
Water, $c_0 = 1447$ m/s
 γ_R in steel = 0.9278

Table VI. Complex roots of dispersion relation in thick-plate theory corresponding to symmetric waves in unloaded plate.

| UNLOADED PLATE | | | LOADED PLATE | | | | | |
|----------------|----------|---------|---|---|---|---|--|---|
| kd | γ | $k_g d$ | A+S, loaded one side | | S only, loaded one side | | S only, loaded both sides | |
| | | | Re($\Delta\gamma$) | Im($\Delta\gamma$) | Re($\Delta\gamma$) | Im($\Delta\gamma$) | Re($\Delta\gamma$) | Im($\Delta\gamma$) |
| 0.5 | 1.6841 | 0.84205 | -8.321×10^{-5} $\pm 7 \times 10^{-8}$ | 1.5173×10^{-3} $\pm 7 \times 10^{-8}$ | -3.016×10^{-5} $\pm 4 \times 10^{-8}$ | 1.5183×10^{-3} $\pm 4 \times 10^{-8}$ | 5.25×10^{-6} $\pm 7 \times 10^{-8}$ | 3.0361×10^{-3} $\pm 7 \times 10^{-8}$ |
| 0.9 | 1.6601 | 1.49409 | -6.44×10^{-5} $\pm 2 \times 10^{-7}$ | 3.3452×10^{-3} $\pm 2 \times 10^{-7}$ | 2.3×10^{-6} $\pm 2 \times 10^{-7}$ | 3.3447×10^{-3} $\pm 2 \times 10^{-7}$ | 1.532×10^{-4} $\pm 2 \times 10^{-7}$ | 6.6848×10^{-3} $\pm 2 \times 10^{-7}$ |
| 1.3 | 1.6158 | 2.10054 | 4.29×10^{-5} $\pm 2 \times 10^{-7}$ | 6.5198×10^{-3} $\pm 2 \times 10^{-7}$ | 1.389×10^{-4} $\pm 2 \times 10^{-7}$ | 6.5766×10^{-3} $\pm 2 \times 10^{-7}$ | 5.915×10^{-4} $\pm 3 \times 10^{-7}$ | 1.3014×10^{-2} $(\pm 3 \times 10^{-7})$ |
| 1.7 | 1.5465 | 2.62905 | 1.113×10^{-4} $\pm 6 \times 10^{-7}$ | 1.1727×10^{-2} $(\pm 6 \times 10^{-7})$ | 2.614×10^{-4} $\pm 6 \times 10^{-7}$ | 1.1718×10^{-2} $(\pm 6 \times 10^{-7})$ | 1.2672×10^{-3} $\pm 4 \times 10^{-7}$ | 2.3396×10^{-2} $(\pm 4 \times 10^{-7})$ |
| 2.5 | 1.3698 | 3.42450 | -3.288×10^{-4} $\pm 5 \times 10^{-7}$ | 2.0723×10^{-2} $(\pm 5 \times 10^{-7})$ | -5.94×10^{-5} $\pm 3 \times 10^{-7}$ | 2.0714×10^{-2} $\pm 3 \times 10^{-7}$ | 5.346×10^{-4} $\pm 7 \times 10^{-7}$ | 4.1532×10^{-2} $(\pm 7 \times 10^{-7})$ |
| 4.5 | 1.1106 | 4.99770 | -7.476×10^{-4} $\pm 2 \times 10^{-7}$ | 1.3502×10^{-2} $(\pm 2 \times 10^{-7})$ | -5.10×10^{-4} $\pm 3 \times 10^{-7}$ | 1.35×10^{-2} $(\pm 3 \times 10^{-7})$ | -1.0257×10^{-3} $\pm 7 \times 10^{-7}$ | 2.6992×10^{-2} $(\pm 7 \times 10^{-7})$ |
| 6.9 | 1.0124 | 6.98556 | -5.778×10^{-4} $\pm 2 \times 10^{-7}$ | 7.9489×10^{-3} $\pm 2 \times 10^{-7}$ | -3.822×10^{-4} $\pm 2 \times 10^{-7}$ | 7.9425×10^{-3} $\pm 2 \times 10^{-7}$ | 6.043×10^{-4} $\pm 4 \times 10^{-7}$ | 1.588×10^{-2} $(\pm 4 \times 10^{-7})$ |
| 8.1 | 0.9904 | 8.02224 | -5.886×10^{-4} $(\pm 6 \times 10^{-8})$ | 6.5758×10^{-3} $(\pm 6 \times 10^{-8})$ | 4.027×10^{-4} $\pm 1 \times 10^{-7}$ | 6.568×10^{-3} $(\pm 1 \times 10^{-7})$ | 5.593×10^{-4} $\pm 3 \times 10^{-7}$ | 1.3133×10^{-2} $(\pm 3 \times 10^{-7})$ |
| 9.7 | 0.9722 | 9.43034 | -5.785×10^{-4} $\pm 1 \times 10^{-7}$ | 5.3539×10^{-3} $\pm 1 \times 10^{-7}$ | 4.002×10^{-4} $\pm 3 \times 10^{-7}$ | 5.3439×10^{-3} $\pm 3 \times 10^{-7}$ | 5.068×10^{-4} $\pm 3 \times 10^{-7}$ | 1.0687×10^{-2} $(\pm 3 \times 10^{-7})$ |

Table VII. Complex roots of dispersion relation in exact elasticity theory corresponding to symmetric waves in unloaded plate.

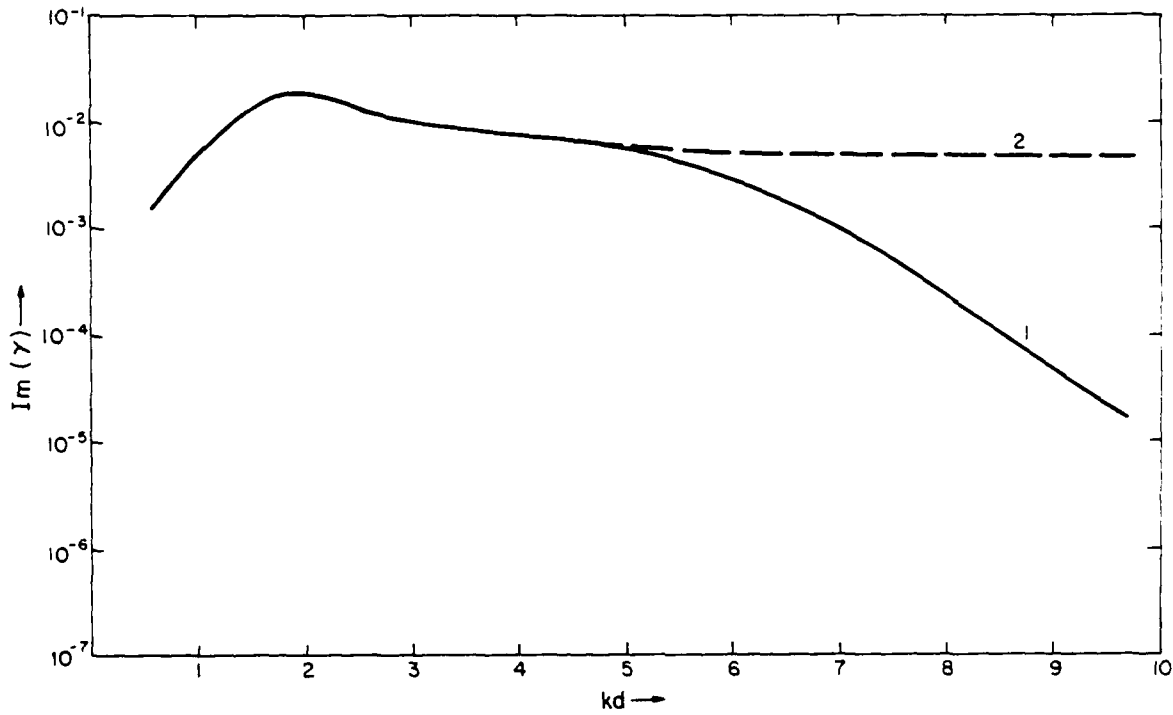
| UNLOADED PLATE | | | LOADED PLATE | | | | | |
|----------------|----------|---------|--|---|--|---|--|---|
| kd | γ | $k_s d$ | A+S, loaded one side | | S only, loaded one side | | S only, loaded both sides | |
| | | | Re($\Delta\gamma$) | Im($\Delta\gamma$) | Re($\Delta\gamma$) | Im($\Delta\gamma$) | Re($\Delta\gamma$) | Im($\Delta\gamma$) |
| 0.5 | 1.6626 | 0.83130 | 1.6869×10^{-2} ($\pm 1 \cdot 10^{-7}$) | 1.5772×10^{-3} $\pm 1 \cdot 10^{-7}$ | 1.6918×10^{-2} ($\pm 1 \cdot 10^{-6}$) | 1.579×10^{-3} ($\pm 1 \cdot 10^{-6}$) | 1.696×10^{-2} $\pm 1 \cdot 10^{-5}$ | 3.17×10^{-3} $\pm 1 \cdot 10^{-5}$ |
| 0.9 | 1.5932 | 1.43388 | 4.6866×10^{-2} ($\pm 2 \cdot 10^{-7}$) | 3.9029×10^{-3} $\pm 2 \cdot 10^{-7}$ | 4.6916×10^{-2} $\pm 7 \cdot 10^{-6}$ | 3.905×10^{-3} $\pm 7 \cdot 10^{-6}$ | 4.7102×10^{-2} $\pm 7 \cdot 10^{-6}$ | 7.974×10^{-3} $\pm 7 \cdot 10^{-6}$ |
| 1.3 | 1.4460 | 1.87980 | 1.1758×10^{-1} ($\pm 8 \cdot 10^{-7}$) | 8.794×10^{-3} ($\pm 8 \cdot 10^{-7}$) | 1.176×10^{-1} ($\pm 6 \cdot 10^{-6}$) | 8.794×10^{-3} $\pm 6 \cdot 10^{-6}$ | 1.1835×10^{-1} $\pm 6 \cdot 10^{-5}$ | 1.756×10^{-2} $\pm 6 \cdot 10^{-5}$ |
| 1.7 | 1.2750 | 2.16750 | 1.7232×10^{-1} ($\pm 6 \cdot 10^{-5}$) | 1.703×10^{-2} $\pm 6 \cdot 10^{-5}$ | 1.7233×10^{-1} $\pm 6 \cdot 10^{-5}$ | 1.701×10^{-2} $\pm 6 \cdot 10^{-5}$ | 1.7394×10^{-1} $\pm 6 \cdot 10^{-5}$ | 3.409×10^{-2} $\pm 6 \cdot 10^{-5}$ |
| 2.5 | 1.1507 | 2.87675 | -7.5078×10^{-2} $\pm 5 \cdot 10^{-6}$ | 1.2996×10^{-2} $\pm 5 \cdot 10^{-6}$ | -7.493×10^{-2} $\pm 5 \cdot 10^{-5}$ | 1.295×10^{-2} $\pm 5 \cdot 10^{-5}$ | -7.513×10^{-2} $\pm 5 \cdot 10^{-5}$ | 2.598×10^{-2} $\pm 5 \cdot 10^{-5}$ |
| 4.5 | 0.9485 | 4.26825 | 3.964×10^{-3} $\pm 6 \cdot 10^{-6}$ | 6.479×10^{-3} $\pm 6 \cdot 10^{-6}$ | 4.53×10^{-3} $\pm 7 \cdot 10^{-5}$ | 6.41×10^{-3} $\pm 7 \cdot 10^{-5}$ | 4.62×10^{-3} $\pm 5 \cdot 10^{-5}$ | 1.28×10^{-2} $\pm 5 \cdot 10^{-5}$ |
| 6.9 | 0.9367 | 6.42183 | -8.92×10^{-3} $\pm 2 \cdot 10^{-6}$ | 1.141×10^{-3} $\pm 2 \cdot 10^{-6}$ | -5.43×10^{-3} $\pm 2 \cdot 10^{-5}$ | 4.98×10^{-3} $\pm 2 \cdot 10^{-5}$ | -5.24×10^{-3} $\pm 2 \cdot 10^{-5}$ | 9.98×10^{-3} $\pm 2 \cdot 10^{-5}$ |
| 8.1 | 0.9290 | 7.52490 | -1.1501×10^{-3} $\pm 3 \cdot 10^{-7}$ | 1.743×10^{-4} $\pm 3 \cdot 10^{-7}$ | 2.3×10^{-4} $\pm 2 \cdot 10^{-5}$ | 4.79×10^{-3} $\pm 2 \cdot 10^{-5}$ | 4.5×10^{-4} $\pm 1 \cdot 10^{-5}$ | 9.57×10^{-3} $\pm 1 \cdot 10^{-5}$ |
| 9.7 | 0.9282 | 9.00354 | -3.50×10^{-4} $\pm 2 \cdot 10^{-6}$ | 1.6×10^{-5} $\pm 2 \cdot 10^{-6}$ | 1.16×10^{-4} $\pm 9 \cdot 10^{-6}$ | 4.671×10^{-3} $\pm 9 \cdot 10^{-6}$ | 3.58×10^{-4} $\pm 1 \cdot 10^{-6}$ | 9.344×10^{-3} $\pm 2 \cdot 10^{-6}$ |



Curve #1 - Antisymmetric and symmetric wave occurring simultaneously.

Curve #2 - Antisymmetric wave only.

Fig. 2. Imaginary part of relative phase speed γ as a function of the dimensionless wave number kd , corresponding to antisymmetric root of the unloaded case. Exact elasticity theory.



Curve #1 - Symmetric and antisymmetric waves occurring simultaneously.

Curve #2 - Symmetric wave only.

Fig. 3. Imaginary part of relative wave speed γ as a function of dimensionless wave number kd , corresponding to symmetric root of the unloaded case. Exact elasticity theory.

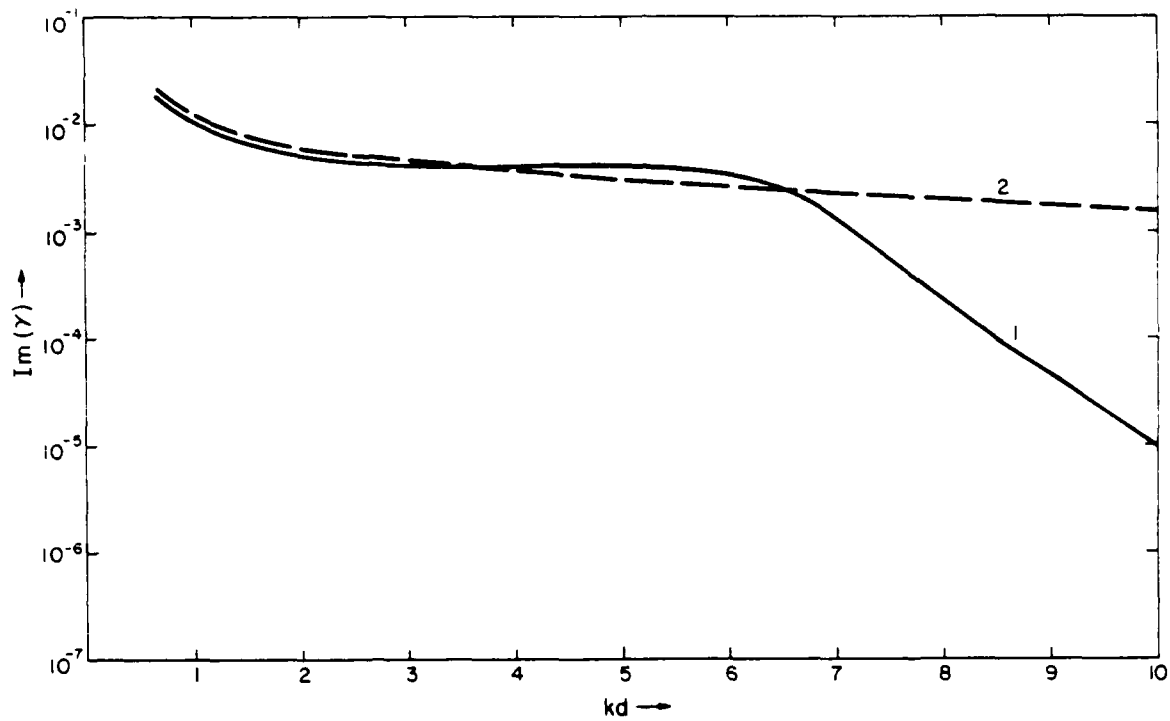


Fig. 4. Comparison of imaginary part of relative phase speed γ as a function of dimensionless wave number kd for exact elasticity theory (Curve #1) and thick-plate theory (Curve #2), for root corresponding to antisymmetric root in unloaded case.

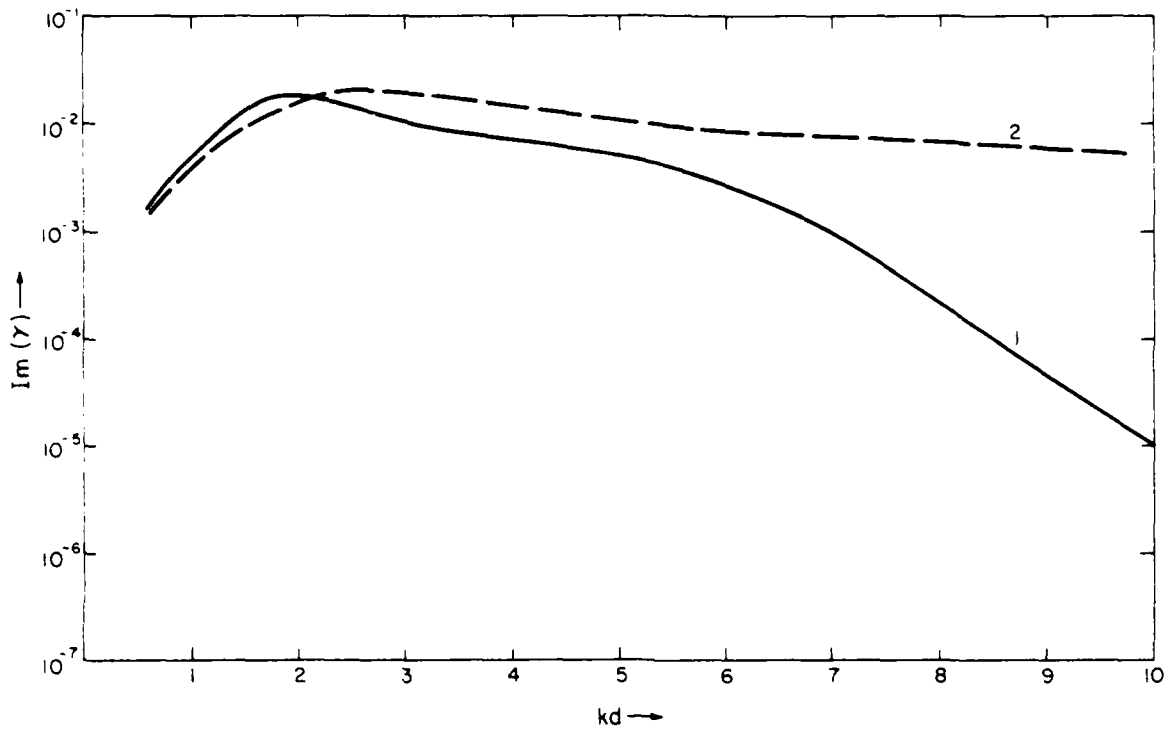


Fig. 5. Comparison of imaginary part of relative phase speed γ as a function of dimensionless wave number kd , for exact elasticity theory (Curve #1) and thick-plate theory (Curve #2), for root corresponding to symmetric root in unloaded case.

APPENDIX A

DESCRIPTION OF ROOT-FINDING PROGRAM

The principle of the complex root finder described in this report is general, but the specific form of the program is adapted to the problem of finding roots of the dispersion relation of straight-crested waves in a fluid-loaded plate. The development of the dispersion relation for such waves is given in the Application section of this report. Flow diagram, list of symbols, source listing, and examples are attached as Appendices B, C, D, and E, respectively.

First the material parameters are entered into the program: POI, Poisson's ratio of the plate material; COCS, the ratio of the sound speed in the fluid to the shear wave speed in the plate; and RHM, the ratio of the fluid density to the density of the plate material. Next, the complex correction factor (AKAR, AKAI) for the effective shear modulus in thick-plate theory is entered, with the (uncritical) value of the step in z , DELZ, used to approximate the derivative $\partial f/\partial z$ (see Complex Root-Finder Program section). Then the frequency is entered in the form of the dimensionless wave number $k_s d$ (AKSD) for shear waves in the plate, with the corresponding dimensionless propagation speed for an unloaded plate, ZNOT, which should be computed by a program for finding real roots [8]. On the same line, a maximum number of iterations are entered, which serves to provide an exit from the program in case it fails to converge. Three control-type variables are entered next: ANR, the number of steps in which the approach from zero density to full density is performed; TOL, the number for the relative accuracy of the final result; and the multiplication factor FSTEP, for the step size in the movement of the test pairs (see Complex Root-Finder Program section). The option number BID chooses from various options, concerning exact theory or thick-plate theory and antisymmetric or symmetric waves and fluid-loading on one side or both sides. The listing of these options is given in Appendix B.

The computations and loops follow closely the discussion of the main algorithm in the Complex Root-Finder Program section. If the program fails to converge, a statement is printed out which indicates an exit left or right or up or down, depending on the direction of motion of the pertinent test pair. The name SIGN refers to the quantity, the algebraic sign of which is the criterion for the location of the root with respect to the test pair. If SIGN is equal to zero, a message to that extent is printed and the program transfers to the end where a return option number is to be entered.

The accuracy of the final answer is determined by the comparison of the larger of the relative errors in the real and imaginary parts of the change

in relative wave speed to the number TOL entered in the program. For every step in the density, an intermediate value of the complex wave speed is printed out. A dimensionless attenuation factor $-(k_2d)$ is computed and printed out that is computed according to

$$-(k_2d) = \frac{(k_S d) \gamma_2}{\gamma_1 + \gamma_2} \quad (A1)$$

where 1,2 refer to the real and imaginary parts of a complex number, k_S is the wave number for shear waves, $2d$ the thickness of the plate, γ_1 and γ_2 are the real and imaginary parts of the dimensionless propagation speed $\gamma = c/c_S$, c is the propagation speed, and c_S is the speed of shear waves in the plate. At the end of the program, a return option number is requested that returns the program to any of the five lines where input data are entered. Typing in zero for the option number results in an exit from the program.

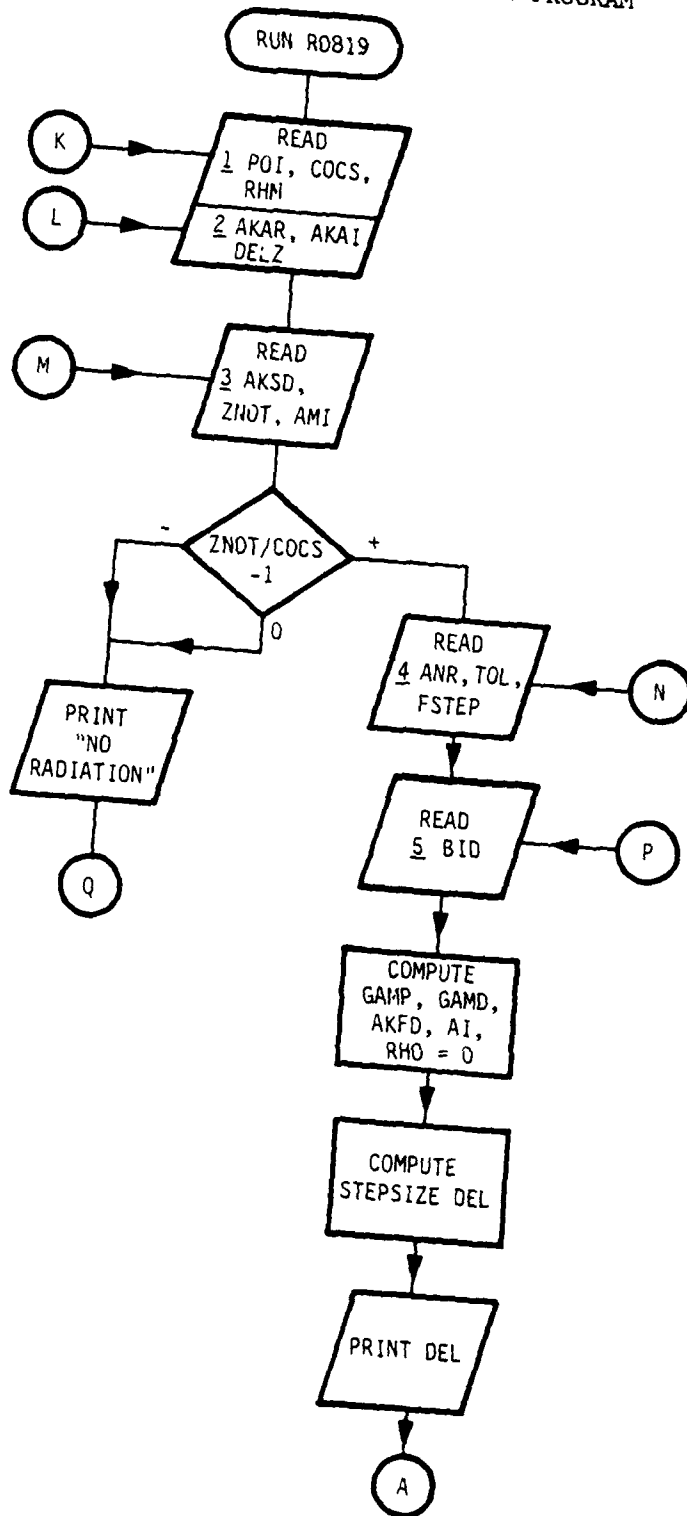
Special caution is due in the use of a complex square-root routine, since the square root is a double-valued function. It occurs several times in the program: first in computation of the quantities q' and s' , defined by $q'^2 = k_d^2 - k^2$, and $s'^2 = k_S^2 - k^2$ [compare Eqs. (14) and (15)]. The two possible roots differ by a factor of -1 , of course. The structure of the dispersion determinant is such that the change from one root to the other introduces a factor of -1 into the determinant value, and thus does not affect the location of zeros of the determinant. The program converges properly as long as one stays with one branch of the function and does not jump from one branch to the other. The FORTRAN subroutine selects always the square root that has a positive real part; if the real part is zero, it selects the positive purely imaginary root. This amounts to a branch cut along the negative real axis in the complex plane of the argument of the function, and this prevented convergence of the program in some cases. The problem was remedied by the following method. If the numerical value for q'^2 or s'^2 has a negative real part, it is multiplied by -1 before the square root is taken. The result is then multiplied by $-i$. This is equivalent to moving the branch cut from the negative real axis to the positive real axis. This should solve the problem in all cases where the root is not close to the origin, as compared with the chosen stepsize.

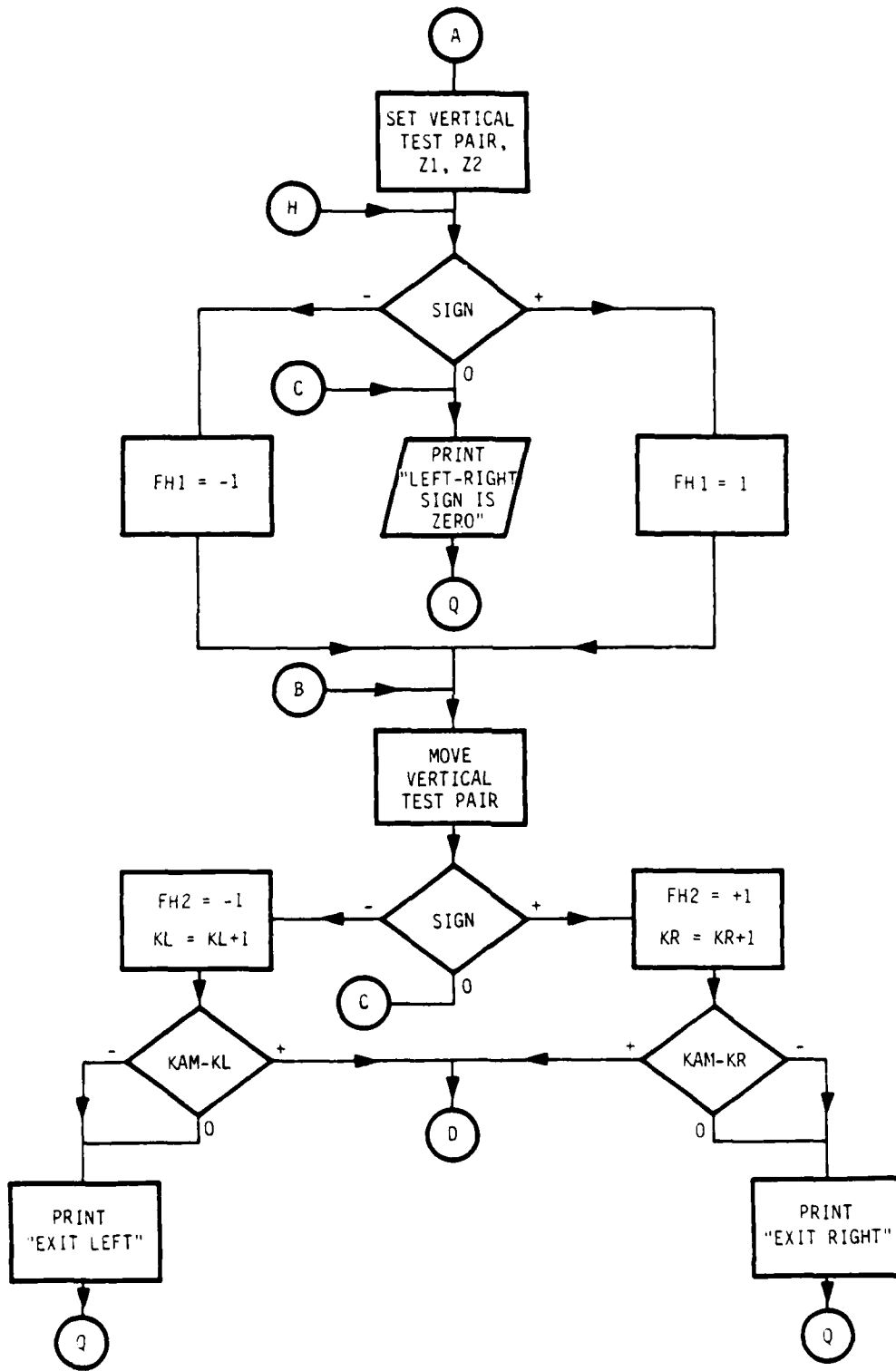
In the second place the square-root routine appears in the calculation of $\cot \theta$, where θ is the angle with the normal to the plate of the radiation emitted into the fluid. It is calculated by the equation $\cot \theta = [(c/c_0)^2 - 1]^{1/2}$, which follows from the coincidence condition between the waves in the plate and in the fluid. Since the imaginary part of the phase speed c is always small compared with the real part, there is no problem in this case with the branch cut of the subroutine, as long as c is larger than c_0 and not very close to c_0 . If $c < c_0$, one has the situation where there is no radiation into the fluid; the factor $[(c/c_0)^2 - 1]^{1/2}$ is purely imaginary, and the root finder is not able to operate. Therefore the program checks for the algebraic sign of the expression $(c/c_0)^2 - 1$ in the beginning, when c has still the value of

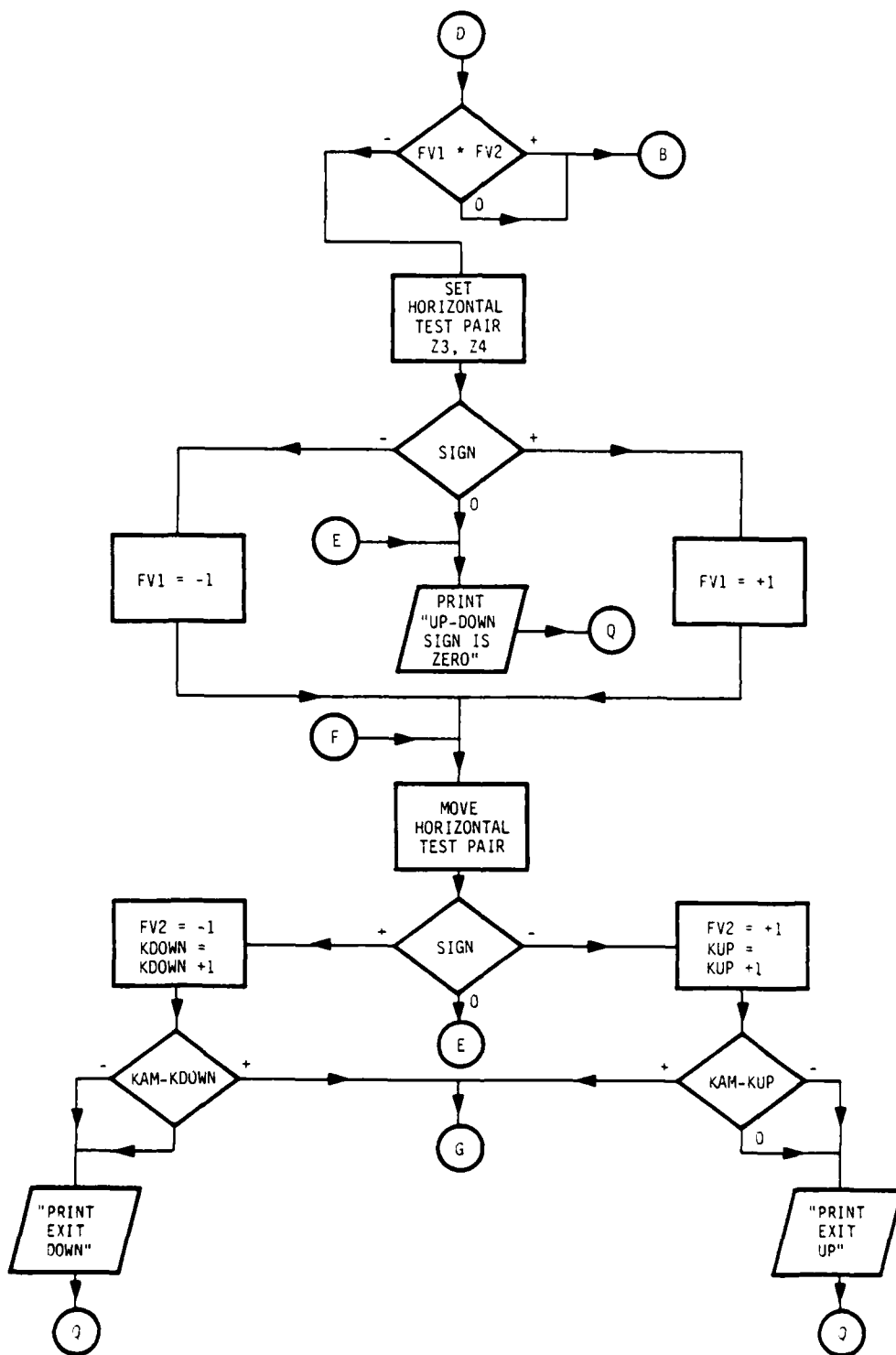
the phase speed for an unloaded plate. If this is negative, the program prints a statement that no radiation into the fluid is possible and moves to the request for a new return option number.

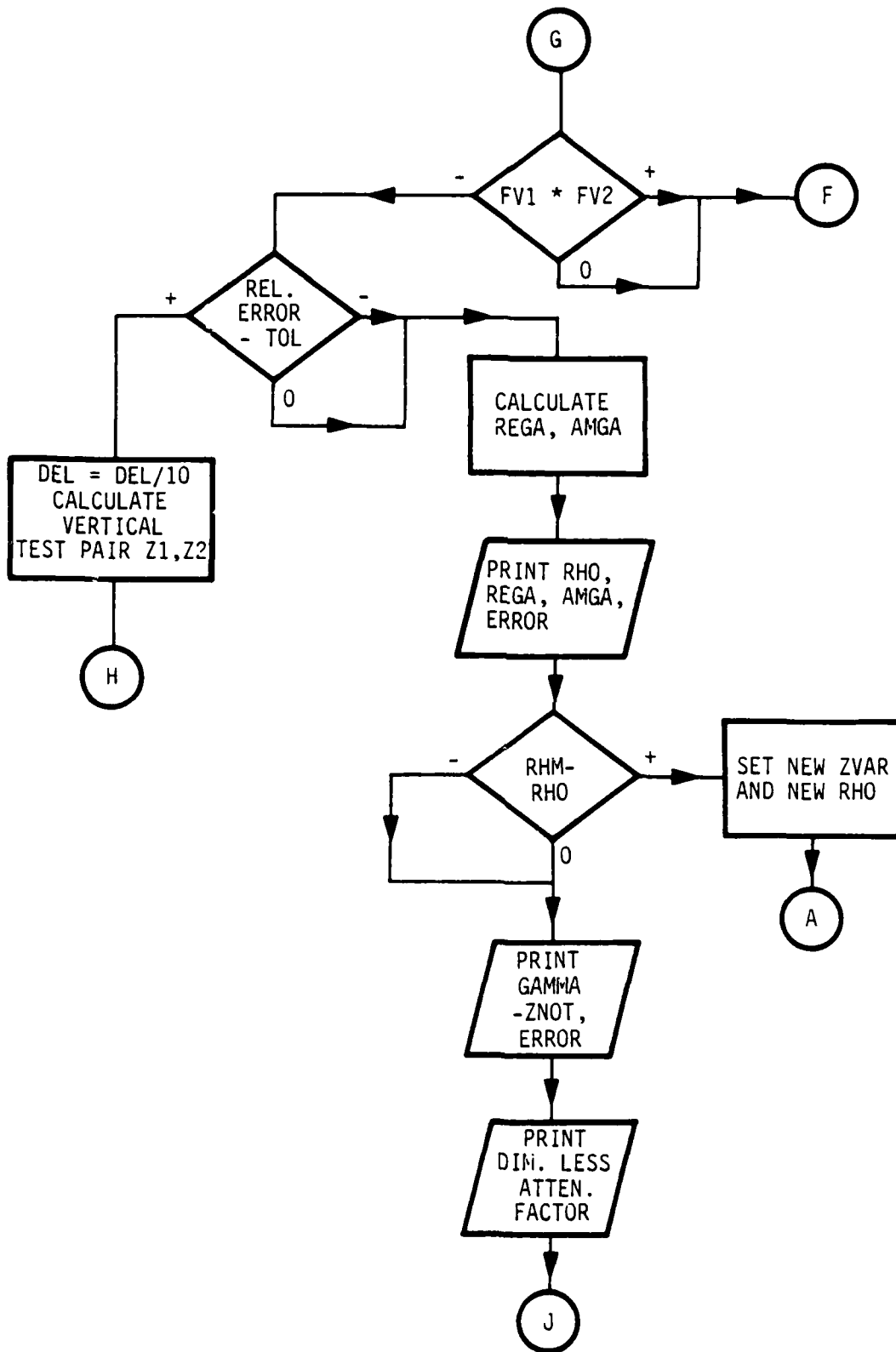
APPENDIX B

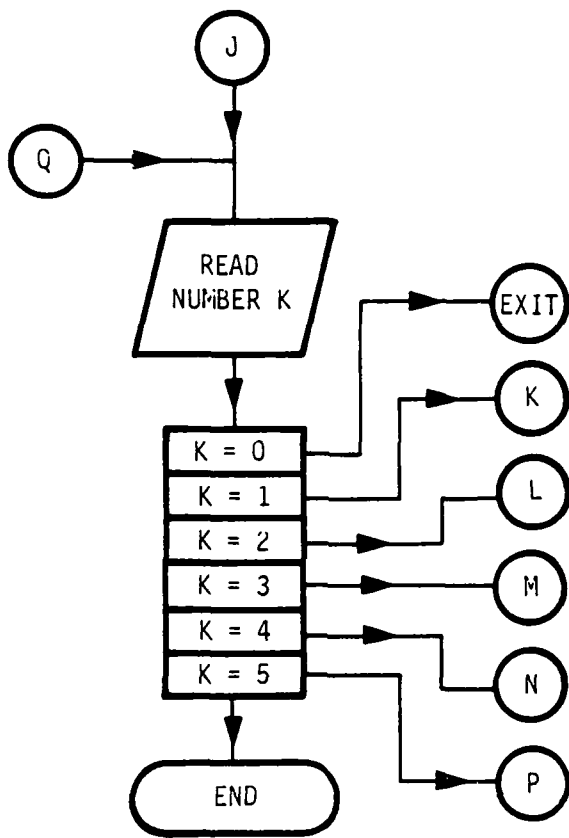
FLOW DIAGRAM R0819 MAIN PROGRAM



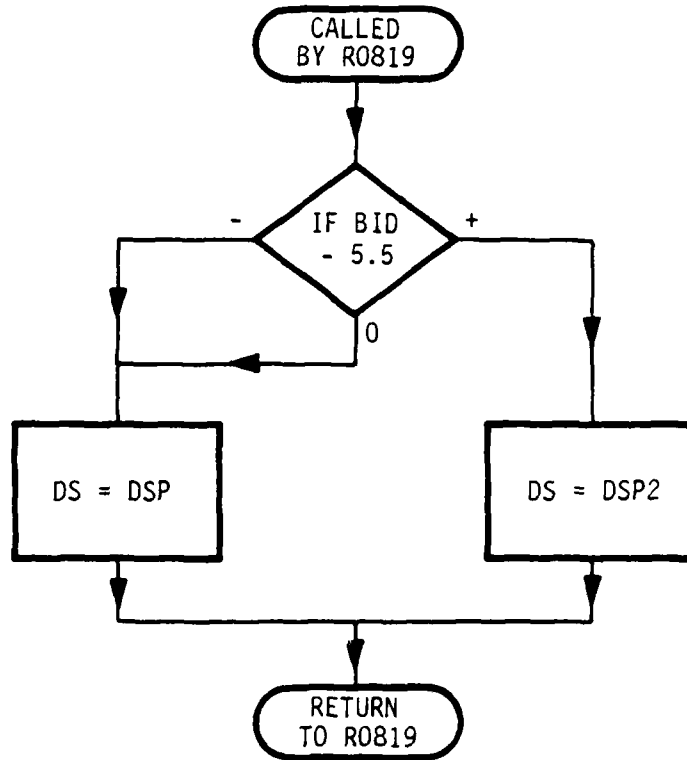




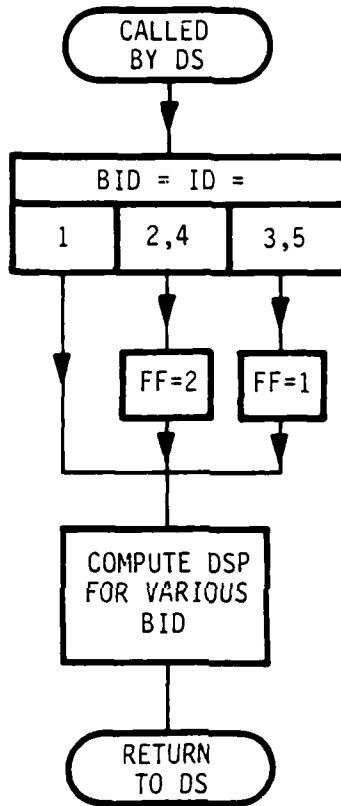




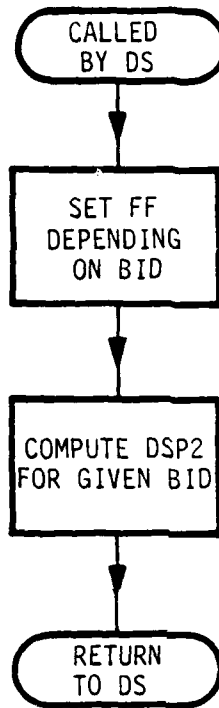
FLOW DIAGRAM FUNCTION SUBPROGRAM DS



FLOW DIAGRAM FUNCTION SUBPROGRAM DSP



FLOW DIAGRAM FUNCTION SUBPROGRAM DSP2



APPENDIX C

LISTING OF MAJOR SYMBOLS IN FORTRAN PROGRAM

| | |
|-----------|--|
| AI | i, imaginary unit |
| AKAP | κ , complex correction factor for shear modulus |
| AKAR | Real part of κ |
| AKAI | Imaginary part of κ |
| AKFD | $k_0 d$, dimensionless wave number in fluid |
| AKSD | $k_s d$, dimensionless wave number for shear waves in plate |
| ANR = NR | Number of steps to reach nominal density RHM |
| AMGA | Imaginary part of wave speed γ |
| AMI = KAM | Number of iterations allowed in loop |
| ATF | $-k_2 d$, where $k_2 = \text{Im}(k)$, dimensionless attenuation factor |
| BID = ID | Number of required option |
| | 1: Thick-plate theory, antisymmetric and symmetric waves, fluid on one side. |
| | 2: Thick-plate theory, antisymmetric wave only, fluid on one side. |
| | 3: Thick-plate theory, antisymmetric wave only, same fluid on both sides. |
| | 4: Thick-plate theory, symmetric wave only, fluid on one side. |
| | 5: Thick-plate theory, symmetric wave only, same fluid on both sides. |
| | 6: Exact theory, antisymmetric and symmetric waves, fluid on one side. |
| | 7: Exact theory, antisymmetric wave only, fluid on one side. |
| | 8: Exact theory, antisymmetric wave only, same fluid on both sides. |
| | 9: Exact theory, symmetric wave only, fluid on one side. |
| | 10: Exact theory, symmetric wave only, same fluid on both sides. |

COCS c_o/c_s , propagation speed in fluid relative to shear wave speed in plate.

DS(Z) Function subprogram calling DSP(Z) or DSP2(Z).

DSP(Z) Function subprogram for dispersion relation in thick-plate theory.

DSP2(Z) Function subprogram for dispersion relation in exact theory.

DFDZ Approximation for $\partial f/\partial z$.

DEL Real step size.

DELZ Δz , used in computation of approximation to $\partial f/\partial z$.

DELP Intermediate symbol for step size DEL.

DELH, DELV Step sizes for movement of test pairs, horizontally and vertically.

DZ Complex step size

F $[(c/c_o)^2 - 1]^{1/2}$

FF Factor in dispersion relation FF = 1, fluid on both sides
FF = 2, fluid on one side

F1,F2,
F3,F4 $f(z_1), f(z_2), f(z_3), f(z_4)$

FV1,FV2,
FH1,FH2 Flags to indicate direction of motion of test pairs.

FSTEP Factor to adjust step size DEL.

GAMD γ_d , phase speed of dilatational waves relative to shear wave speed.

GAMP γ_p , phase speed of extensional waves relative to shear wave speed.

ID = BID

IDSP, IBD Intermediate option numbers.

K Return option number
= 1, program returns to entering POI, COCS, RHM
= 2, program returns to entering AKAR, AKAI, DELZ
= 3, program returns to entering AKSD, ZNOT, AMI
= 4, program returns to entering ANR, TOL, FSTEP
= 5, program returns to entering BID
= 0, program exits.

KAM = AMI

KR, KL,
 KUP, KDOWN Counters in loops to check number of iterations.

NR = ANR

NRV Counter in advancing the parameter RHO.

POI Poisson's ratio.

REGA Real part of relative wave speed γ .

RHM Nominal density of fluid loading the plate, divided by
 density of plate material.

RHO Stepwise varied value of relative density, varying from
 zero to RHM.

QPR $q'd = [(k_d d)^2 - (kd)^2]^{1/2}$, dimensionless wave number.

SIGN Expression, the algebraic sign of which determines location
 of root relative to test pair.

SPR $s'd = [(k_s d)^2 - (kd)^2]^{1/2}$, dimensionless wave number.

TOL Limit for relative error in the root.

Z Variable for root used in calling function subroutines.

Z1, Z2 Vertical test pair.

Z3, Z4 Horizontal test pair.

ZNOT Value for the real root of the dispersion relation without
 fluid loading, from a real root finder, serving as the
 seed for starting the program.

ZVAR Intermediate value of root, serving as seed for the next
 step in the parameter RHO.

APPENDIX D

SOURCE PROGRAM LISTING

```

COMPLEX Z, DSP, AI, DFDZ, DZ, ZVAR, Z1, Z2, Z3, Z4, F1, F2, F3, F4, DSP2
COMPLEX AKAF, DS, CMPLX
COMMON RHO, AKSD, GAMP, GAMD, AKAR, AKAI, AKFD, ID, IDSP
1 WRITE (5,30)
30 FORMAT(' $ENTER POI, COCS, RHM: ')
READ (5,39) POI, COCS, RHM
39 FORMAT(3F15.0)
2 WRITE (5,31)
31 FORMAT(' $ENTER AKAR, AKAI, DELZ: ')
READ (5,39) AKAR, AKAI, DELZ
AKAF=CMPLX(AKAR, AKAI)
11 WRITE (5,50)
50 FORMAT(' $ENTER AKSD, ZNOT, # OF IT.: ')
READ (5,39) AKSD, ZNOT, AMI
IF (ZNOT/COCS-1.) 61, 61, 62
61 WRITE (5,63)
63 FORMAT (' NO RADIATION INTO FLUID')
GO TO 100
62 KAM=AMI
10 WRITE (5,45)
45 FORMAT (' $ENTER ANR, TOL, FSTEP: ')
47 READ (5,39) ANR, TOL, FSTEP
12 WRITE (5,33)
33 FORMAT (' $ENTER BID: ')
8 READ (5,8) BID
FORMAT (F15.0)
ID=BID
AI=CMPLX(0., 1.)
GAMP=SQRT(2./(1.-POI))
GAMD=SQRT(2.*(1.-POI)/(1.-2.*POI))
AKFD=AKSD/COCS
RHO=0.
NR=INT(ANR)
NRV=0
C COMPUTE STEPSIZE DEL
ZVAR=ZNOT
Z=ZVAR+DELZ
DFDZ=DS(Z)/DELZ
RHO=RHO+RHM/ANR
NRV=NRV+1
DZ=-DS(ZVAR)/DFDZ
X=ABS(REAL(DZ))
Y=ABS(AIMAG(DZ))
DEL=AMAX1(X, Y)*FSTEP
WRITE(5,301) DEL

```

```

301  FORMAT(' DEL= .E12.5')
      DELP=DEL
C     FIND INITIAL DIRECTION OF MOVEMENT OF
C     VERTICAL TEST PAIR
70    DEL=DELP
64    Z1=ZVAR-AI*DEL
      Z2=ZVAR+AI*DEL
65    F1=DS(Z1)
      F2=DS(Z2)
      KR=0
      KL=0
      KUP=0
      KDOWN=0
      SIGN=AIMAG(F1)*REAL(F2)-REAL(F1)*AIMAG(F2)
      IF(SIGN)71,72,73
71    FH1=-1.
      GO TO 74
72    WRITE(5,302)
302   FORMAT (' LEFT-RIGHT SIGN = ZERO')
      GO TO 100
73    FH1=1.
74    DELH=FH1*DEL
C     LOOP TO FIND VERTICAL LINES BRACKETING ROOT
75    Z1=Z1+DELH
      Z2=Z2+DELH
      F1=DS(Z1)
      F2=DS(Z2)
      SIGN=AIMAG(F1)*REAL(F2)-AIMAG(F2)*REAL(F1)
      IF (SIGN) 81,72,83
81    FH2=-1.
      KL=KL+1
      IF (KAM-KL) 99,99,84
99    WRITE(5,310)
310   FORMAT (' EXIT LEFT')
      GO TO 100

83    FH2 = 1.
      KR=KR+1
      IF(KAM-KR) 98,98,84
98    WRITE (5,311)
311   FORMAT(' EXIT RIGHT')
      GO TO 100
84    IF (FH1*FH2) 92,75,75
C     FIND INITIAL DIRECTION OF MOVEMENT
C     OF HORIZONTAL TEST PAIR
92    Z4=(Z1+Z2)/2.+DEL
      KR=0
      KL=0
      Z3=(Z1+Z2)/2.-DEL
      F3=DS(Z3)
      F4=DS(Z4)
      SIGN=AIMAG(F3)*REAL(F4)-AIMAG(F4)*REAL(F3)
      IF (SIGN) 101,102,103

```

```

101      FV1=1.
        GO TO 104
102      WRITE (5,304)
304      FORMAT(' UP-DOWN SIGN = ZERO ')
        GO TO 100
103      FV1=-1.
104      DELV=FV1*DEL
C      LOOP TO FIND HORIZONTAL LINES BRACKETING ROOT
105      Z4=Z4+AI*DELV
        Z3=Z3+AI*DELV
        F3=DS(Z3)
        F4=DS(Z4)
        SIGN=AIMAG(F3)*REAL(F4)-AIMAG(F4)*REAL(F3)
        IF (SIGN) 111,102,113
111      FV2 =1.
        KUP=KUP+1
        IF(KAM-KUP) 97,97,114
97      WRITE(5,305)
305      FORMAT (' EXIT UP')
        GO TO 100
113      FV2=-1.
        KDOWN=KDOWN+1
        IF (KAM-KDOWN) 96,96,114
96      WRITE(5,306)
306      FORMAT(' EXIT DOWN')
        GO TO 100
114      IF (FV1*FV2) 122,105,105
122      REGA=REAL(Z1)
        AMGA=AIMAG(Z3)
        KUP=0
        KDOWN=0
133      AMGA=ABS(AMGA)
        DREG=ABS(REGA-ZNOT)
C      CHECK IF REQUIRED PRECISION IS REACHED
        IF (DEL/AMIN1(DREG,AMGA)-TOL) 132,132,131
131      CONTINUE
        DEL=DEL/10.
        Z1=(Z3+Z4)/2.-AI*DEL
        Z2=(Z3+Z4)/2.+AI*DEL
        GO TO 65
132      REGA=REAL (Z1) -DELH/2.
        AMGA=AIMAG(Z3)-DELV/2.
        DELH=ABS(DELH/2.)
C      PRINT PRELIMINARY RESULTS FOR INTERMEDIATE RHO
        WRITE(5,140) RHO,REGA,AMGA,DELH
140      FORMAT(' RHO,REGA,AMGA,DELH=',2F10.6,2E15.5)
C      CHECK IF FINAL RHO HAS BEEN REACHED
        IF(NR-NRV)145,145,146
146      ZVAR=REGA+AMGA*AI
        RHO=RHO+RHM/ANR
        NRV=NRV+1
        GO TO 70

```

```

145      GO TO (701,702,802,703,803,704,705,805,706,806,707) IN
701      WRITE(5,711)
        GO TO 707
702      WRITE(5,712)
        GO TO 707
802      WRITE(5,812)
        GO TO 707
703      WRITE (5,713)
        GO TO 707
803      WRITE (5,813)
        GO TO 707
704      WRITE (5,714)
        GO TO 707
705      WRITE(5,715)
        GO TO 707
805      WRITE(5,815)
        GO TO 707
706      WRITE (5,716)
        GO TO 707
806      WRITE (5,816)
707      CONTINUE
C      COMPUTE ATTENUATION FACTOR
        ATF=AKSD*AMGA/(REGA**2+AMGA**2)
711      FORMAT(' THICK PLATE, A. AND S., FLUID ONE SIDE')
712      FORMAT(' THICK PLATE, A.ONLY, FLUID ONE SIDE')
812      FORMAT(' THICK PLATE, A.ONLY, FLUID BOTH SIDES')
713      FORMAT(' THICK PLATE, S.ONLY, FLUID ONE SIDE')
813      FORMAT(' THICK PLATE, S.ONLY, FLUID BOTH SIDES')
714      FORMAT(' EXACT, A. AND S., FLUID ONE SIDE')
715      FORMAT(' EXACT, A.ONLY, FLUID ONE SIDE')
815      FORMAT(' EXACT, A ONLY, FLUID BOTH SIDES')
716      FORMAT(' EXACT, S. ONLY, FLUID ONE SIDE')
816      FORMAT(' EXACT, S. ONLY, FLUID BOTH SIDES')
171      FORMAT (2F10.6)
        WRITE (5,172) AKSD,ZNOT
172      FORMAT(' VALUES OF AKSD,ZNOT, ARE ',2F10.6)
        WRITE (5,173)
173      FORMAT(' REAL AND IM. PARTS OF GAMMA-ZNOT AND ERROR ARE')
        REGA=REGA-ZNOT
        WRITE (5,174)REGA,AMGA,DELH
174      FORMAT(3E15.5)
        WRITE(5,175) ATF
175      FORMAT (' DIMENSIONLESS ATTEN.FACTOR = ',E12.5)
100      WRITE (5,159)
159      FORMAT ('$ENTER RETURN OPTION NUMBER ')
        READ (5,151) K
151      FORMAT (I4)
        GO TO (1,2,11,10,12) K
        END

```

```

FUNCTION DS(Z)
COMPLEX DS,DSP,Z,DSP2,AKAF
COMMON RHO,AKSD,GAMP,GAMD,AKAR,AKAI,AKFD,ID,IDSP
BID=ID
IF(BID-5.5)50,50,60
50 DS=DSP(Z)
GO TO 70
60 DS=DSP2(Z)
70 RETURN
END

```

```

FUNCTION DSP(Z)
COMPLEX DSP,AI,AKAF
COMPLEX A11,A22,S11,S22,DELA,DELS,Z,F,CMPLX,CSQRT
COMMON RHO,AKSD,GAMP,GAMD,AKAR,AKAI,AKFD,ID,IDSP
GO TO (7,6,5,6,5) ID
5 FF=1.
GO TO 7
6 FF=2.
7 CONTINUE
AI=CMPLX(0.0,1.0)
AKAF=CMPLX(AKAR,AKAI)
A11=AKSD**2*(Z**2-GAMP**2)/3.-AKAF**2*Z**2
A22=AKSD**2*(AKAF**2-Z**2)
DELA=A11*A22+AKSD**2*Z**2*AKAF**4
S11=AKSD**2*(GAMD**2-Z**2)
S22=AKSD**2*(AKAF**2-Z**2)/3.+(GAMD*Z)**2
DELS=S11*S22-(AKSD*Z*(GAMD**2-2.))**2
F=CSQRT((Z*AKFD/AKSD)**2-1.)
GO TO (10,20,20,30,30) ID
10 DSP=AI*DELA*DELS-Z**3*AKSD*RHO/2.)*(DELA*S11+DELS*A11)/F
GO TO 40
20 DSP=AI*DELA-Z**3*AKSD*RHO*A11/(F*FF)
GO TO 40
30 DSP=AI*DELS-Z**3*AKSD*RHO*S11/(F*FF)
40 RETURN
END

```

```

FUNCTION DSP2(Z)
COMPLEX DSP2,AI,A11,A22,S11,S22,AKD,SFR,QFR,AKAF,D1,D2,D3
COMPLEX DELA,DELS,Z,F,CMPLX,CSQRT,CCOS,CSIN
COMPLEX CCQ,CSQ,CSS,CCS
COMMON RHO,AKSD,GAMP,GAMD,ANAR,AKAI,AKFD,FD,FD5F
IBD=ID-5
FF=2.
GO TO (7,6,5,6,5) IBD
5   FF=1.
   GO TO 7
6   FF=2.
7   CONTINUE
   AI=CMPLX(0.,1.)
   AKD=AKSD/Z
   IF (REAL(AKD**2-AKSD**2)) 11,12,12
12  SPR=-AI*CSQRT(AKD**2-AKSD**2)
   GO TO 13
11  SPR=CSQRT(AKSD**2-AKD**2)
13  IF (REAL(1.-(Z/GAMD)**2)) 21,22,22
21  QPR=CSQRT((Z/GAMD)**2-1.)*AKD
   GO TO 23
22  QPR=-AI*CSQRT(1.-(Z/GAMD)**2)*AKD
23  A11=(AKD**2-SPR**2)*CSIN(QPR)
   A22=-(AKD**2-SPR**2)*CCOS(SFR)
   DELA=A11*A22-4.*AKD**2*QPR*SPR*CSIN(SFR)*CCOS(QPR)
   S11=(AKD**2-SPR**2)*CCOS(QPR)
   S22=-(AKD**2-SPR**2)*CSIN(SFR)
   DELS=S11*S22-4.*AKD**2*QPR*SPR*CSIN(QPR)*CCOS(SFR)
   F=CSQRT((Z*AKFD/AKSD)**2-1.)
   D1=DELA*DELS*AI
   D2=RHO*QPR*AKSD**4*DELS*CCOS(QPR)*CCOS(SFR)/(AKD*F)
   D3=RHO*QPR*AKSD**4*DELA*CSIN(QPR)*CSIN(SFR)/(AKD*F)
   GO TO (15,25,25,35,35) IBD
15  DSP2=D1+(D3-D2)/FF
   GO TO 45
25  DSP2=D1-D2/FF
   GO TO 45
35  DSP2=D1+D3/FF
45  CONTINUE
   RETURN
   END

```

APPENDIX E

EXAMPLES

Items 1 and 2 show two examples where the running of the program took place without complications. In Item 3 the program fails to converge, conceivably due to the close proximity of another root of the dispersion relation, originating in a symmetric real root. This example shows how increasing ANR, which is the number of steps to reach the full value of the density of the fluid, does result in convergence of the program.

```

RUN R0819

1  ENTER POI,COCS,RHM: .3028,.44332,.12806
   ENTER ANR, AKAI, DELZ: .9278,0.0,0.01
   ENTER AKSD,ZNOT,# OF IT.:4.05135,.9003,200.
   ENTER ANR, TOL, FSTEP: 1.,0.01,1.
   ENTER BID: 2.
   DEL= 0.33621E-02
   RHO,REGA,AMGA,DELH= 0.128060 0.900309 0.33512E-02 0.16810E-07
   THICK PLATE, A.ONLY, FLUID ONE SIDE
   VALUES OF AKSD,ZNOT, ARE 4.051350 0.900300
   REAL AND IM. PARTS OF GAMMA-ZNOT AND ERROR ARE
     0.90003E-05 0.33512E-02 0.16810E-07
   DIMENSIONLESS ATTEN.FACTOR = 0.16750E-01
   ENTER RETURN OPTION NUMBER 3

2  ENTER AKSD,ZNOT,# OF IT.:5.9423,.9142,200.
   ENTER ANR, TOL, FSTEP: 1.,0.01,1.
   ENTER BID: 2.
   DEL= 0.23942E-02
   RHO,REGA,AMGA,DELH= 0.128060 0.914153 0.23979E-02 0.11971E-06
   THICK PLATE, A.ONLY, FLUID ONE SIDE
   VALUES OF AKSD,ZNOT, ARE 5.942300 0.914200
   REAL AND IM. PARTS OF GAMMA-ZNOT AND ERROR ARE
     -0.47207E-04 0.23979E-02 0.11971E-06
   DIMENSIONLESS ATTEN.FACTOR = 0.17051E-01
   ENTER RETURN OPTION NUMBER 3

3  ENTER AKSD,ZNOT,# OF IT.:7.81745,.9197,200.
   ENTER ANR, TOL, FSTEP: 1.,0.01,1.
   ENTER BID: 2.
   DEL= 0.18673E-02
   EXIT LEFT
   ENTER RETURN OPTION NUMBER 4

   ENTER ANR, TOL, FSTEP: 3.,0.01,1.
   ENTER BID: 2.
   DEL= 0.62245E-03
   RHO,REGA,AMGA,DELH= 0.042687 0.919709 0.61999E-03 0.31122E-07
   RHO,REGA,AMGA,DELH= 0.085373 0.919708 0.12400E-02 0.31122E-07
   EXIT RIGHT
   ENTER RETURN OPTION NUMBER 4

```

```

ENTER ANR, TOL, FSTEP: 5.,0.01,1.
ENTER BID: 2.
DEL= 0.37347E-03
RHO,REGA,AMGA,DELH= 0.025612 0.919709 0.37199E-03 0.18673E-07
RHO,REGA,AMGA,DELH= 0.051224 0.919709 0.74399E-03 0.18673E-07
RHO,REGA,AMGA,DELH= 0.076836 0.919708 0.11160E-02 0.18673E-07
RHO,REGA,AMGA,DELH= 0.102448 0.919707 0.14880E-02 0.18673E-07
RHO,REGA,AMGA,DELH= 0.128060 0.919705 0.18600E-02 0.18673E-07
THICK PLATE, A.ONLY, FLUID ONE SIDE
VALUES OF AKSD,ZNOT, ARE 7.817450 0.919700
REAL AND IM. PARTS OF GAMMA-ZNOT AND ERROR ARE
0.50664E-05 0.18600E-02 0.18673E-07
DIMENSIONLESS ATTN.FACTOR = 0.17190E-01
ENTER RETURN OPTION NUMBER 0

```

The next example shows that in some cases increase of ANR or increasing FSTEP can make the program converge. It is not clear whether or not there are cases where one of these two variables would induce convergence and not the other.

RUN R0819

ENTER POI,COCS,RHM: .3028,.4432,.12806
 ENTER AKAR, AKAI, DELZ: .9278,0.0,0.01
 ENTER AKSD,ZNOT, OF IT.:7.5249,.9290,200.
 ENTER ANR, TOL, FSTEP: 3.,0.01,1.
 ENTER BID: 6.

DEL= 0.54452E-03
 RHO,REGA,AMGA,DELH= 0.042687 0.927811 0.64525E-03 0.27226E-05
 RHO,REGA,AMGA,DELH= 0.085373 0.927847 0.26817E-03 0.27226E-06
 RHO,REGA,AMGA,DELH= 0.128060 0.927850 0.17425E-03 0.27226E-06
 EXACT, A. AND S., FLUID ONE SIDE
 VALUES OF AKSD,ZNOT, ARE 7.524900 0.929000
 REAL AND IM. PARTS OF GAMMA-ZNOT AND ERROR ARE
 -0.11500E-02 0.17425E-03 0.27226E-06
 DIMENSIONLESS ATTEN.FACTOR = 0.15230E-02
 ENTER RETURN OPTION NUMBER 5

ENTER BID: 9.
 DEL= 0.58163E-03
 EXIT LEFT
 ENTER RETURN OPTION NUMBER 4

ENTER ANR, TOL, FSTEP: 10.,0.01,1.
 ENTER BID: 9.

DEL= 0.17449E-03
 RHO,REGA,AMGA,DELH= 0.012806 0.929164 0.47871E-03 0.87244E-07
 RHO,REGA,AMGA,DELH= 0.025612 0.929167 0.95742E-03 0.87244E-07
 RHO,REGA,AMGA,DELH= 0.038418 0.929170 0.14361E-02 0.87244E-07
 RHO,REGA,AMGA,DELH= 0.051224 0.929175 0.19148E-02 0.87244E-07
 RHO,REGA,AMGA,DELH= 0.064030 0.929182 0.23938E-02 0.87244E-06
 RHO,REGA,AMGA,DELH= 0.076836 0.929190 0.28728E-02 0.87244E-06
 RHO,REGA,AMGA,DELH= 0.089642 0.929200 0.33517E-02 0.87244E-06
 RHO,REGA,AMGA,DELH= 0.102448 0.929212 0.38290E-02 0.87244E-06
 RHO,REGA,AMGA,DELH= 0.115254 0.929224 0.43079E-02 0.87244E-06
 RHO,REGA,AMGA,DELH= 0.128060 0.929237 0.47869E-02 0.87244E-06
 EXACT, S. ONLY, FLUID ONE SIDE
 VALUES OF AKSD,ZNOT, ARE 7.524900 0.929000
 REAL AND IM. PARTS OF GAMMA-ZNOT AND ERROR ARE
 0.23711E-03 0.47869E-02 0.87244E-06
 DIMENSIONLESS ATTEN.FACTOR = 0.41715E-01
 ENTER RETURN OPTION NUMBER 4

ENTER ANR, TOL, FSTEP: 3.,0.01,3.
 ENTER BID: 9.

DEL= 0.17449E-02
 RHO,REGA,AMGA,DELH= 0.042687 0.929172 0.15958E-02 0.87244E-07
 RHO,REGA,AMGA,DELH= 0.085373 0.929196 0.31915E-02 0.87244E-06
 RHO,REGA,AMGA,DELH= 0.128060 0.929237 0.47872E-02 0.87244E-06
 EXACT, S. ONLY, FLUID ONE SIDE
 VALUES OF AKSD,ZNOT, ARE 7.524900 0.929000
 REAL AND IM. PARTS OF GAMMA-ZNOT AND ERROR ARE
 0.23729E-03 0.47872E-02 0.87244E-06
 DIMENSIONLESS ATTEN.FACTOR = 0.41717E-01
 ENTER RETURN OPTION NUMBER 0

END

DATE
FILMED

1 - 82

DTIC